SCIENCE FACULTY

PhD PROGRAM IN

SCIENCE

MENTION NEUROSCIENCE

ENDOCANNABINOID SIGNALING MEDIATE SYNAPTIC PLASTICITY FROM SOMATOSTATIN-EXPRESSING GABAERGIC NEURONS IN THE PREFRONTAL CORTEX

Nicole Sanguinetti González

Thesis to opt for PhD Degree in Sciences

Mention Neuroscience

Thesis Director:

Dra. Chiayu Chiu

2025

Table of Contents

LIST OF FIGURES AND TABLES

ABBREVIATIONS

ACSF: Artificial cerebroespinal fluid
AEA: Anandamide
2-AG: 2- arachidonoylglycerol
AM251: Inverse agonist of cannabinoid type 1 receptors
AP: Action Potential
BAPTA: 1,2-bis (o-aminophenoxy) ethane-N, N, N′, N'-tetraacetic acid
CB1R: Cannabinoid receptor type 1
CB2R: Cannabinoid receptor type 2
CNS: Central Nervous System
CCK: Cholecystokinin
ChR2: Channelrhodopsin-2
DGL: Diacylglycerol lipase
DSE: Depolarization-induced suppression of excitation
DSI: Depolarization-induced suppression of inhibition
EPSC: Postsynaptic Excitatory Current
eCBs: Endocannabinoids
GDPβS: Guanosine-5'-(β-thio)-diphosphate
5HT: 5-hydroxytryptamine
5HT3AR: Serotonin 5HT3A receptor
5HT2R: Serotonin type 2 receptor
IN: Interneurons
IPSC: Postsynaptic Inhibitory Current
KO: Knockout
LTD: Long-Term Depression
LTP: Long-Term Potentiation
MCPG: (+)-alpha-Methyl-4-carboxyphenylglycine
mGluR-I: Group I metabotropic glutamate receptors
NBQX: 2,3-dioxo-6-nitro-7-sulfamoyl-benzo[f]quinoxaline
TBS: Theta-burst stimulation
TCB2: (7R)-3-bromo-2, 5-dimethoxy-bicyclo [4.2.0] octa-1,3,5-trien-7-yl] methanamine
THC: Tetrahydrocannabinol
PFC: Prefrontal Cortex
PPR: Paired Pulse Ratio
PN: Pyramidal Neuron
PKA: Protein kinase A
PV: Parvalbumin peptide
PLC: Phospholipase C
Ritanserine: 5H- [1,3] thiazolo[3,2-a] pyrimidin-5-one
SOM: Somatostatin peptide
STD: Short-Term Depression
VIP: Peptide intestinal vasoactive
VGCCs: Voltage gated Ca^{2+} channels
WIN: Agonist of cannabinoid type 1 receptors

ABSTRACT

GABAergic interneurons (INs) that co-express the neuropeptide somatostatin (SOM-INs) play an essential role in controlling cortical activity by forming inhibitory synapses on dendrites of pyramidal neurons (PNs). However, the mechanisms that regulate inhibition from SOM-INs are less understood. Given commonalities between SOM-INs and the endocannabinoid (eCB) system in influencing cognitive and emotional processing, we examine the possibility that GABAergic synapses from SOM-INs can be modulated by eCB signaling in the prefrontal cortex (PFC). Using optogenetic tools to selectively activate SOM-INs in whole-cell patch experiments, we found that postsynaptic inhibitory currents (IPSC) in layer II/III PNs evoked by photostimulation of SOM-INs (SOM-IPSCs) depressed following bath application of WIN 55,212-2, a potent agonist of cannabinoid type 1 receptors (CB1Rs). Supporting the role of CB1Rs in presynaptic neurotransmitter release, WIN depression from SOM-INs was accompanied by changes in paired-pulse ratio (PPR) and is absent in mice lacking CB1Rs specifically in SOM-INs (SOM-CB1R KOs). Importantly, a brief postsynaptic depolarization of the PNs induced suppression of inhibition transiently (DSI), an effect that was eliminated by the CB1R inverse agonist AM251. Moreover, theta-burst stimulation (TBS) triggered long-term depression from SOM-INs (iLTD) that was blocked by AM251 and was absent in SOM-CB1R KO animals. Consistent with a presynaptic expression of TBS-iLTD, we observed a decrease in PPR from SOM-IPSCs following plasticity induction. In addition, WIN and TBS have no effect on IPSCs mediated by photostimulating parvalbumin-expressing interneurons (PV-INs), suggesting that inhibition from PV-INs is not regulated by eCB signaling. Altogether, these results reveal an input-specific eCB modulation from SOM-INs, a major source of dendritic inhibition in the PFC, to potentially control information flow from multiple sources to shape associative cognitive processing.

INTRODUCTION

Communication between neurons is the cellular basis of thinking and movement control. Information processing in normal brain function requires balanced activity between excitatory and inhibitory cells (E-I balance). Disruption of this E-I balance has been linked to several neuropsychiatric disorders, including schizophrenia, autism, and epilepsy (Kano et al., 2009; Di Marzo et al., 2015). eCBs, powerful regulators of neural activity throughout the central nervous system (CNS) (Castillo et al., 2012), have been suggested to contribute to maintaining and disrupting E-I balance. Indeed, eCB signaling plays key roles in short-term and long-term plasticity at excitatory and inhibitory synaptic transmission in numerous brain regions (Chevaleyre et al., 2006). In PFC, alterations in eCB system have been associated with neuropsychiatric disorders that reflect PFC dysfunction, and preclinical data has demonstrated that eCB signaling is important in regulating stress, emotional processing, and cognitive functions (Sewell et al., 2009; Hillard et al., 2012).

THE ENDOCANNABINOID SYSTEM

The eCB system comprises the eCBs such as anandamide (AEA) and 2- arachidonoylglycerol (2-AG) (Devane et al., 1992; Mechoulam, 1995), the cannabinoid type 1 and type 2 receptors (CB1Rs and CB2Rs), the enzymes responsible for eCB synthesis and metabolism, and transporters that regulate eCB levels in the synaptic cleft (Howlett et al., 2002). eCBs are a group of lipid molecules that get their name from the exogenous cannabinoid Δ9-tetrahydrocannabinol (Δ9-THC), the main psychoactive component in cannabis (Castillo et al., 2012). They are produced on demand via increased intracellular Ca^{2+} at postsynaptic sites in response to prolonged synaptic activity (Chevaleyre et al., 2006; Heifets & Castillo, 2009). AEA and 2-AG are the most prominent eCBs (Kano et al., 2009). Both are derivatives of arachidonic acid (Zou & Kumar, 2018), but they differ in their biosynthesis and degradation pathways, as well as affinity for receptor binding (Augustin

& Lovinger, 2018). 2-AG is considered a major eCB given that it is found at high concentrations in the brain and is an efficacious eCB ligand, acting as a specific cannabinoid receptor agonist (Mechoulam, 1995; Sugiura et al., 2002). The synthesis of 2-AG occurs through the phosphoslipase (PLC) β- diacylglycerol lipase (DGL) pathway after the activation of Gq/11-coupled receptors such as the muscarinic M1/M3 or group I metabotropic glutamate (mGluR-I) receptors (Sugiura et al., 2002;Zou & Kumar, 2018). PLCβ hydrolyzes phosphatidylinositol to generate diacylglycerol, which is converted to 2-AG by diacylglycerol lipase α (DGLα) specifically localized in postsynaptic compartments (Katona et al., 2006; Lafourcade et al., 2007). Interestingly, 2-AG production can also be triggered by Ca^{2+} influx via voltage gated Ca^{2+} channels (VGCCs), although the precise mechanisms are unknown. There are two enzymes that metabolizes 2-AG, monoacylglycerol lipase (MGL) that is found more heterogeneously across synapses (Tanimura et al., 2012) and controls the duration and magnitude of 2-AG-mediated synaptic plasticity (Hashimotodani et al., 2007) and serine hydrolase ABHD6 that is located postsynaptically and catabolizes a small fraction of 2-AG (Marrs et al., 2010).

THE CANNABINOID RECEPTORS

The CB1R is expressed predominantly in the CNS, whereas the CB2R is mostly present peripherally in the immune system (Munro et al., 1993). Both are seven transmembrane receptors that are coupled to the pertussis toxin sensitive G protein, Gi/o (Howlett et al., 2002). Activation of either cannabinoid receptor reduces adenylyl cyclase (AC) activity, thus lowering cAMP levels and protein kinase A (PKA) activity. CB1Rs are present at presynaptic and axonal compartments, restricting their function to sites of synaptic activity (Mackie, 2005; Bodor et al., 2005; Hashimoto et al., 2008). In addition, it binds to synthetic cannabimimetic compounds such as CP55940, JWH-015, WIN55212-2 and the endogenous compounds AEA and 2-AG (Howlett et al., 2002). The CB1R is one of the most highly expressed G protein-coupled receptors in the brain (Herkenham

et al., 1990) and is widely distributed in many brain areas embodying the cortico-limbic system like prefrontal cortex, hippocampus, cerebellum, striatum, and amygdala (Katona et al., 2001). In these areas, CB1Rs are present in many different cell types, where their expression levels are variable. Notably, cortical GABAergic presynaptic terminals contain high levels of the CB1R protein, whereas PNs have lower levels of these receptors (Busquets-Garcia et al., 2018). Nevertheless, the high expression of CB1Rs at presynaptic terminals suggests a role of eCBs in the regulation of synaptic efficacy and neuronal activity (Augustin & Lovinger, 2018).

ENDOCANNABINOID SIGNALING IN THE CNS

The eCB system is one of the key regulatory mechanisms in the brain controlling multiple events such as mood, pain perception, learning and memory among others (Marsicano & Lutz, 1999; Kano et al., 2009). It is also thought to provide a neuroprotective role during traumatic brain injury (TBI) and may be part of the natural brain compensatory repair mechanism during neurodegeneration (Pryce et al., 2003; Campbell & Gowran, 2007; Bilkei-Gorzo, 2012). The principal mechanism by which eCBs acts in the brain is by regulating synaptic function through retrograde signaling, as observed in short-term and long-term forms of synaptic plasticity (Chevaleyre et al., 2006) that contribute to learning and memory (Marsicano et al., 2002; Kishimoto & Kano, 2006). eCBs are released from neurons in an activity-dependent manner, act retrogradely on presynaptic CB1Rs and modulate transmitter release (Alger, 2002). eCB mobilization can be triggered either by strong neuronal depolarization (Ohno-shosaku et al., 2002) or by activation of phospholipase Cβ (PLCβ) (Hashimotodani et al., 2005) through Gq-coupled receptors such as group I metabotropic glutamate receptors (mGluR-I), M1/M3 muscarinic acetylcholine receptors, and serotonin type 2 receptors (5HT2R) (Maejima et al., 2001; Fukudome et al., 2004) (see Figure 1). In addition, eCBs act in non-retrograde ways, activating postsynaptic CB1Rs and/or the transient receptor potential vanilloid type 1 (TRPV1), which are involved in the

transduction of remarkably diverse stimuli, including temperature, pH, mechanical and osmotic pressure, taste, xenobiotic substances, and endogenous lipids (Venkatachalam & Montell, 2007). Moreover, eCBs can signal via astrocytes by triggering gliotransmission to indirectly modulate presynaptic or postsynaptic function (Castillo et al., 2012). The eCB system underlies several short- and long-term forms of synaptic plasticity at both excitatory and inhibitory synapses in several brain areas (Kano et al., 2009). Short-term depression (STD) is commonly triggered by depolarization of the postsynaptic cell, leading to a short-lived calcium dependent mobilization of eCBs and transient CB1R activation. This process is called depolarization-induced suppression of inhibition (DSI) or excitation (DSE) depending on the inhibitory or excitatory nature of the target synapse (Alger, 2002). The mechanism involves direct G protein-dependent inhibition of presynaptic Ca^{+2} influx through VGCCs (Brown et al., 2003) or facilitation of inward-rectifying K^{+} (IRK) channels. eCB-mediated long-term depression (eCB-LTD) is most initiated following repetitive glutamatergic synaptic activity and involves modulation of the presynaptic vesicular release machinery (Heifets & Castillo, 2009). The predominant mechanism of this form of plasticity requires inhibition of AC and downregulation of the cAMP/PKA pathway via the α i/o limb (Heifets & Castillo, 2009). CB1Rs are needed during the induction phase of eCB-LTD that requires combined presynaptic firing with CB1R activation (Heifets et al., 2008). The expression phase of eCB-LTD involves presynaptic proteins Rab3B/RIM1a (Chevaleyre et al., 2007) or a reduction of VGCCs (Mato et al., 2007). The induction of eCB-LTD has been described in several brain regions at both excitatory synapses (E-LTD) and inhibitory synapses (I-LTD) (Heifets & Castillo, 2009). These forms of plasticity are thought to be the cellular basis of learning and memory.

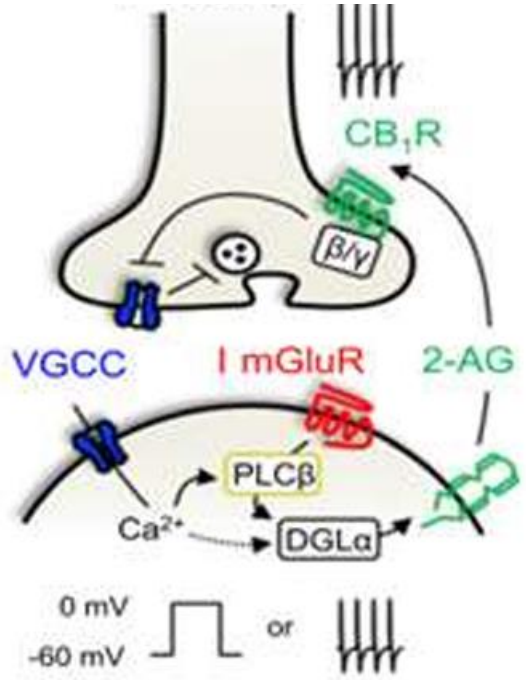

Figure 1. Molecular mechanisms underlying endocannabinoid-mediated synaptic plasticity. Postsynaptic activity triggers Ca^{2+} influx through voltage-gated Ca^{2+} channels (VGCCs), with additional Ca^{2+} contributions from NMDARs and internal stores. This Ca^{2+} influx facilitates diacylglycerol lipase (DGLα)-mediated endocannabinoid (eCB) production by an unknown mechanism. Presynaptic activity can also induce eCB mobilization by activating postsynaptic group I metabotropic glutamate receptors (I mGluRs). Phospholipase Cβ (PLCβ) acts as a coincidence detector, integrating pre- and postsynaptic activity. DGLα promotes the release of 2-arachidonoylglycerol (2-AG), which retrogradely targets presynaptic CB1 receptors (CB1Rs). The βγ subunits are likely coupled to presynaptic VGCCs, reducing neurotransmitter release. (Adapted from Castillo et al., 2012)

ENDOCANNABINOID AT INHIBITORY SYNAPSES

Studies of synaptic plasticity have largely focused on changes to excitatory glutamatergic connections, including both long-term depression and potentiation. Less is known about the plasticity of inhibitory GABAergic synapses in the mammalian brain where these connections exhibit diverse forms of long-term plasticity. Activation of CB1Rs in neocortex has been shown to suppress inhibitory transmission by reducing GABA release (Hill et al., 2007; Galarreta et al., 2008). Interestingly repeated stimulation of the spine facilitated the formation of a GABAergic bouton on the same dendrite. This dendritic feedback signal depended on the postsynaptic activation of DAGL, leading to the production of the endocannabinoid 2-AG, and was mediated through CB1 receptors (Hu et al., 2019). Thus, although CB1Rs are abundantly expressed in the PFC, little is known about the specific neural circuits through which eCBs signal and how eCBs regulate PFC function. eCB-mediated synaptic plasticity at GABAergic synapses is most well-known for the cholecystokinin-expressing (CCK-) INs in the hippocampus (Tsou & Mackie, 1999; Araque et al., 2017;Kepecs & Fishell, 2014; Földy et al., 2006). However, recent work suggests three principal groups of INs in the cortex: cells co-expressing either the Ca^{2+} binding protein parvalbumin (PV), the neuropeptide somatostatin (SOM), or the ionotropic serotonin 5HT3A receptor (5HT3AR) (Rudy et al., 2011). PV-INs account for ~40% of GABAergic neurons and include fast spiking basket cells and chandelier cells. SOM-INs represent ~30% of GABAergic neurons and include the Martinotti cells, a set of neurons that target distal dendritic regions. The 5HT3AR group accounts for ~30% of the total IN population and includes the CCK-INs (see Figure 2).

Figure 2. Reciprocal Connectivity between Interneuron Populations. Three primary subtypes of neocortical inhibitory interneurons are interconnected in a recurring motif of reciprocal inhibition. The strength of these interactions is depicted by the size of the circles representing synaptic connectivity (Adapted from Cardin, 2018). The Ca^{2+}-binding protein parvalbumin (PV), the neuropeptide somatostatin (SST), and the ionotropic serotonin receptor 5HT3a (5HT3aR) account for nearly 100% of neocortical interneurons. The 5HT3aR group, which also accounts for ~30% of the total interneuron population, is heterogeneous and includes all the neurons that express the neuropeptide VIP and CCK-INs (Rudy et al., 2011).

Considering that CCK-INs represent a small percentage of the GABAergic population in the PFC, the impact of the eCB system on PFC function is unclear. We wondered whether inhibition from GABAergic cells other than CCK-INs are under eCB regulation in the PFC. Because most GABAergic synapses are made on postsynaptic dendrites (Bacci et al., 2004; Katona et al. 2000), where they regulate the integration of incoming excitatory synaptic signals. We aimed to investigate the ability of eCBs to modulate synaptic transmission from SOM-INs, a major population of dendrite-targeting INs in the prefrontal cortex. The rich diversity of GABA-producing cell types mediates widely distributed and precisely positioned inhibition. The specific subdomain of GABAergic contact (e.g. dendrite, soma, or axon) critically determines the impact of synaptic inhibition in shaping neuronal activity in the neocortex. SOM-INs primarily target distal dendrites of excitatory neurons (Mcgarry et al., 2010) where they regulate Ca^{2+} signaling, synaptic integration, and dendritic spiking (Chiu et al., 2013). These GABAergic cells mediate feedback inhibition, being most excited by local cortical pyramidal cells. Immunohistochemical evidence suggests that at least 63% of SOM-INs co-express CB1Rs in the cortex (Hill et al., 2007), and in the rat hippocampus, a higher percentage of co-localization between CB1Rs and somatostatin has been reported (Zou & Kumar, 2015). Therefore, we hypothesize that SOM-INs express CB1Rs and be another cellular target by which eCBs exert control over synaptic inhibition.

HYPOTHESIS:

"eCBs modulate GABAergic synaptic transmission from SOM-INs in the PFC."

GENERAL AIM

Elucidate the cellular and circuit mechanisms where eCB- regulate cortical inhibition from SOM-expressing interneurons and the functional impact on cortical function.

SPECIFIC AIM:

1. Determine how eCBs regulate synaptic inhibition from SOM-INs.

1.1. Assess the requirement for CB1R activation in inhibition.

1.2. Evaluate the role of eCBs in Short-Term Depression (STD)

1.3. Evaluate the role of eCBs in Long-Term Depression (LTD)

2. Investigate the cellular mechanism involved in synaptic plasticity mediate by eCBs

2.1. Evaluate the requirement of calcium and group 1 metabotropic glutamate receptors (I-mGluRs) in synaptic plasticity.

2.2. Evaluate the role of neuromodulators in eCBs production.

3. Investigate the consequence of CB1R loss in SOM-INs of PFC.

3.1. Confirm the absent of CB1R in SOM-INs by pharmacology drugs.

3.2. Evaluate the impact of SOMCB1KO in inhibitory and excitatory synapses.

3.3. Evaluate intrinsic properties and synaptic changes in SOMCB1KO mice.

GENERAL METHODS:

Animals

Wild type and transgenic mice strain C57bl6 (e.g., SOM-Cre, SOM-CB1KO knockout, and PV-Cre) from both sexes were used. All experiments were performed on postnatal day (P) 21-35. Mice, born and raised in the animal facility of the Universidad de Valparaiso were maintained at 25°C under a 12h light/dark cycle with water and food ad libitum. All animal protocols were approved by the Bioethical Evaluation Act CBC 59-2022 of the Universidad de Valparaiso, in accordance with the bioethics and biosafety regulations of the Chilean Research Council (CONICYT).

Genotyping Protocol

Founder lines for the conditional CB1R mice were a kind gift from Dr. Eric Delpire (Vanderbilt University, Tennessee USA). They were genotyped by PCR with primers for floxed cnr1 (Forward:5′TGGCTCCTGTCTGCAAGTATAGG3′;

Rev:5′ACTCAAAATGTCCATGTCTTATAACCAG-3′, 400 bp amplicon). PCR conditions were 0.4 µM primer and cycle: 95 °C 3 min; [95 °C 15 s, 62 °C 15s, 72 °C 15 s] × 30 cycles; 72 °C 1 min. Homozygous conditional CB1R female mice were bred with heterozygous SOM-Cre male mice (JAX 005359, Jackson Laboratories, Bar Harbor, ME, USA) to generate mice in which the CB1R was deleted from INs and their control littermates. We developed a double PCR assay for CRE and somatostatin as internal control (IC). CRE primers were CRE-forward:5′-CGGTCGATGCAACGAGTGATG-3 ′; CRE-reverse:5′-AGCCTGTTTTGCACGTTCACC-3′, amplicon bp. IC primers were IC- forward: 5′-CTGGAAGACATTCACATCCTG-3′; IC-reverse:5′-TATGGCAGCTGTTCCCAATAG-3′, amplicon 200-465 bp. Double PCR used 0.4 µM primer and cycle: 95 °C 3 min; [95 °C 15 s, 62 °C 15 s, 72 °C 15 s] × 30 cycles; 72 °C 1 min. Amplicons were run on 2% agarose electrophoresis in TBE buffer (pH 8.4).

Slice Preparation

Experiments were performed in acute prefrontal cortical slices (300 μm thick) taken from male and female mice (P21-P35). Either SOM-Cre mice and offspring of crosses between SOM-Cre and flox-cnr1 mice were used. Coronal slices were cut in ice cold external solution containing (in mM): 110 choline, 25 NaHCO3, 1.25 NaH2PO4, 2.5 KCl, 7 MgCl2, 0.5 CaCl2, 20 glucose, 11.6 sodium ascorbate and 3.1 sodium pyruvate, bubbled with 95% O2 and 5% CO2 and transferred to artificial cerebrospinal fluid (ACSF) containing (in mM): 127 NaCl, 25 NaHCO3, 1.25 NaH2PO4, 2.5 KCl, 1 MgCl2, 2 CaCl2 and 20 glucose bubbled with 95% O2 and 5% CO2. Slices were incubated for 30 min at 34°C and maintained at 20–22°C before use.

Electrophysiology and Analysis

Experiments were conducted at 20–22°C, in a submersion type recording chamber. Whole-cell patch-clamp recordings were obtained from layer 2/3 pyramidal cells (200-300 μm from the pial surface) identified with video-infrared/differential interference contrast. For current-clamp recordings, cortical cells in layer 2/3 were patched using glass pipettes (4-7 MΩ resistance) made from borosilicate glass capillaries. Pipettes were filled with internal solutions containing (in mM): 130 KMeSO3, 10 HEPES, 4 MgCl2, 4 Na2ATP, 0.4 NaGTP and 10 sodium creatine phosphate, adjusted to pH 7.3 with KOH. For voltage-clamp recordings, we used cesium internal solution to improve space clamp. The recording was made from visually identified pyramidal-shaped somata of principal neurons in layer 2/3 PFC. In general aim 1 and 2, IPSCs from SOM or PV-INs were evoked by optogenetic means. In the specific aim 1.1, the magnitude of the WIN effect was calculated as the percentage change between baseline (averaged responses for 5 minutes before drug application) and 25–30 minutes after the start of drug application to the bath. The paired-pulse ratio (PPR) was defined as the ratio of the amplitude of the second IPSC over the amplitude of the first IPSC. To obtain the amplitude of the second IPSC, the first IPSC waveform was first

subtracted from the paired-pulse responses in all experiments where we calculated the PPR. In the specific aim 1.2 and 1.3, Short-Term depression (STD) and Long-Term Depression (LTD) were performed by voltage-clamp recordings with high Cl- internal solution to recorded IPSC, that contained (in mM): 30 CsGluconate, 100 CsCl, 10 HEPES, 4 MgCl2, 4 Na2ATP, 0.4 NaGTP and 10 sodium creatine phosphate, adjusted to pH 7.3 with CsOH. For STD experiments we clamped pyramidal cells at -65mV and we recorded 10 minutes of baseline. After baseline, we delivered 5 seconds of depolarizing step (from -65mV to 0mV), to induce STD. For LTD experiments, we clamped pyramidal cells at -65mV and we recorded 6 minutes of baseline. After baseline, we depolarized the cell from -65mV to +10 mV while we applied a theta burst protocol (TBS), that consists of stimulation of layer 1 (a train of five stimuli at 100 Hz x10). After TBS protocols, cells return to -65mV and were recorded for 30 minutes. In general aim 3, IPSCs and EPSCs were evoked by a monopolar electrode positioned within layer 1 of the PFC and recorded pyramidal cells of layer 3/2 PFC. Cells were clamped at -65mV to isolate EPSC, or +10mV to isolate IPSCs. In addition to corroborating that the current observed are excitatory or inhibitory, we added 50 μM picrotoxin or 10 μM NBQX respectively to the ACSF. IPSCs and EPSCs were evoked with an interstimulus interval of 20 ms at 0.1 Hz. For specific aim 3.3, we delivered 5 pulses at 50Hz, and pyramidal cells were recorded in current clamp to evaluate integration action potential (APs), we analyzed the probability to evoke APs at 30V and at the half-intensity for each cell. The probability of evoking APs was calculated with the number of APs by 6 sweeps for each cell.

All the electrophysiological recordings were made using a Multiclamp 700B amplifier, filtered at 4 kHz, and digitized at 10 kHz. Data will be analyzed in IgorPro software.

ChR2 expression and activation

To optogenetically stimulate SOM-Cre or SOM-CB1R KO and PV-CRE interneurons, mice were injected at P25-30 with AAV-DIO-Ef1α-ChR2-EYFP (UNC Vector Core). Acute cortical slices were prepared for 2-3 weeks post-injection. To activate ChR2, we were overfilling the back aperture of the microscope objective (60x, 1.0 NA) with collimated light from a 455-nm LED light source (ThorLabs).

Statistical Analysis

Data are expressed as the Mean ± S.E.M. Statistical analyses were performed with GraphPad Prism version 8.0.1 (GraphPad Software). We compared independent sample means using t-tests (paired and unpaired t-test), one-way ANOVA and two-way ANOVA as appropriate. We confirmed necessary parametric test assumptions using the Shapiro-Wilk test (normality). $P< 0.001$, $P< 0.01$ and $P< 0.05$ were considered to indicate statistical significance. Sample size for each experiment is indicated in the figure legend for each experiment.

Drugs

WIN 55,212-2, picrotoxin, D-APV, NBQX, BAPTA, GDPβS, AM251, 5-HT, TCB2, Ritanserin were purchased from Sigma Aldrich. (S)-MCPG were obtained from FLUKA. Total DMSO in the bath solution was maintained at 0.1% or below in all experiments.

RESULTS

1. Determine how eCBs regulate synaptic inhibition from SOM-INs.

1.1. Assess the requirement for CB1R activation in inhibition.

In the cortical regions of the mammalian brain, CB1Rs are expressed in the axon terminals of GABA interneurons that contain the neuropeptide cholecystokinin (CCK-INs), where their activation suppresses GABA release (Tsou & Mackie, 1999). However, given that CCK-INs represent a small percentage in the cortex, it remains unclear whether inhibition mediated by other IN subtypes are also under eCB control. To determine whether other INs are sensitive to CB1R activation in PFC, we used 5uM of WIN-55,212-2 (WIN), a CB1R agonist. To this end, we patched clamp PNs and recorded light evoked-IPSC from SOM-INs or PV-INs for 6 minutes as baseline. After baseline, WIN was added to the bath solution in the chamber recording. We observed that WIN suppresses synaptic inhibition from SOM-INs and not from PV-INs (the second class of INs described) (Rudy et al., 2011) onto L2/3 pyramidal neurons in acute bran slices of PFC, confirming a cell-type specific response and sensitivity of SOM-INs to CB1R activation (Figure 3). The IPSC depression by WIN from SOM-INs was 56.5 ± 14.49 % compared to baseline (n=6, p=0.0159). WIN effects in the IPSC from SOM-INs were significant after 30 minutes of WIN application compared to PV-Cre (n=7, $p < 0.0001$, unpaired t test). We also calculated paired pulse ratio (PPR) at an inter-stimulus interval of 100ms. We found significant difference in SOM-Cre after WIN application in PPR analysis (n=7, p= 0.0006, paired t-test), without changes in PV-Cre (n=6, p= 0.2675, paired t-test) (Figure 3).

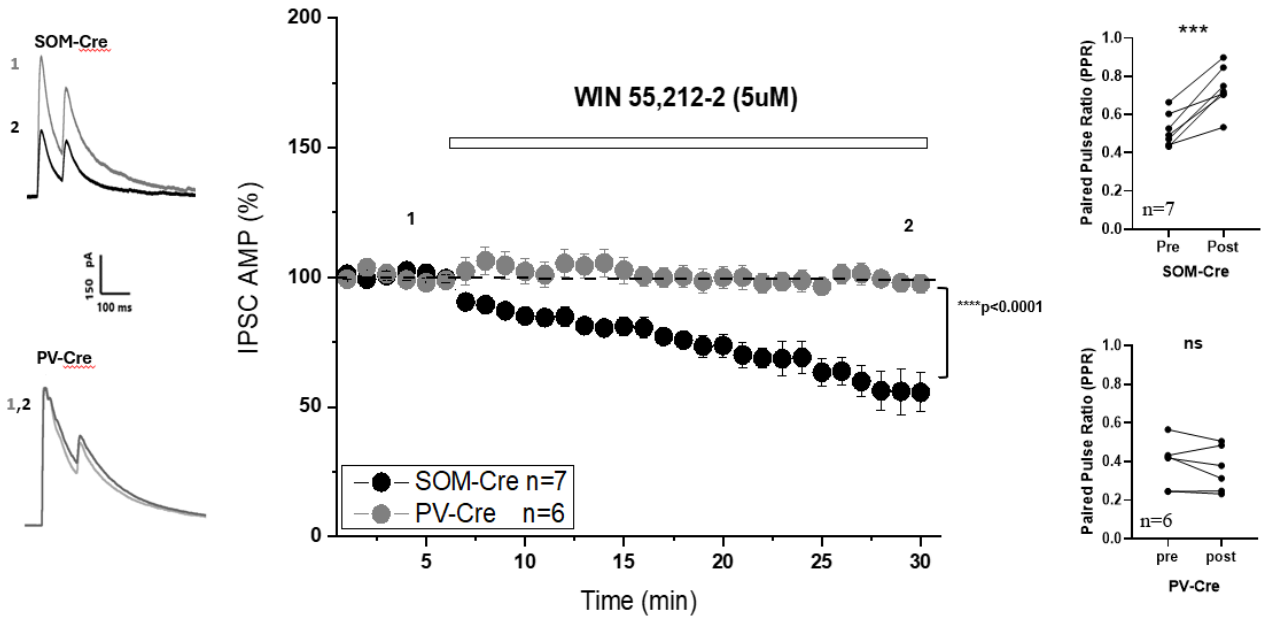

Figure 3. WIN 55,212-2 decreases IPSC amplitude from SOM-INs. Left: Representative traces of inhibitory response from SOM-Cre and PV-Cre on pyramidal cells using ChR2 stimulation before and after WIN application. Middle: WIN effects on the IPSC amplitude mediate by SOM-INs and PV-INs onto pyramidal cells over time. WIN effects in SOM-INs were significant after 30min of WIN application compared with PV-INs, as tested by unpaired test ($p < 0.0001$). Right: Paired pulse ratio (PPR) in SOM-INs and PV-INs before and after WIN application. Significant differences were found in SOM-Cre and no difference in PV-Cre as tested by paired t-test. Bars indicate the standard error. Amplitude is normalized to 10 minutes of baseline for each single experiment. Bars indicate the standard error.

Given that WIN is a non-selective synthetic CB1R agonist, we used AM251, an inverse agonist of CB1R, to confirm whether CB1Rs are required to suppress IPSC from SOM-INs onto PNs. 8uM of AM251 were added in pre-incubate brain slices for 15 minutes. After incubation with AM251, slices were put into the bath solution of chamber recordings to patch PNs and to record IPSC from SOM-INs after light stimulation, for 6 minutes as baseline. After baseline, we added 5uM of WIN to the bath solution, while PNs were patched and recorded light evoked-IPSC from SOM-INs to study WIN effect in pre-incubated slices with AM251. We observed that AM251 prevents IPSC reduction produced by WIN applications compared to control group (without AM251) (Figure 4), confirming that CB1R activation is required to mediate inhibition from SOM-INs onto PNs. WIN effects were significant after 30 min of WIN application in the light evoked-IPSC from SOM-INs, in the control group (n=7), compared to AM251 condition (n=7, $p < 0.0001$, unpaired t-test). In the PPR analysis, we found significant difference in the control group after WIN application (n=7, $p= 0.0076$, paired t-test), without changes in AM251condition (n=7, $p=0.2379$; paired t-test) (Figure 4), suggesting presynaptic mechanism.

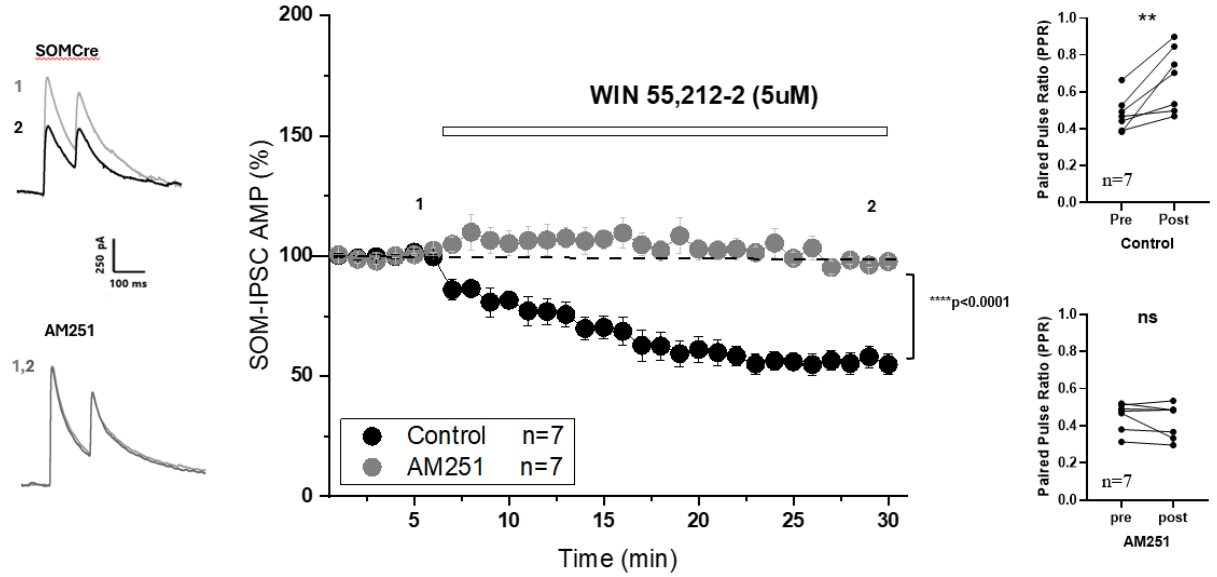

Figure 4. WIN 55,212-2 effects on IPSC amplitude are blocked by AM251. Left: Representative traces of inhibitory response on pyramidal cells from SOM-Cre and AM251 condition, using ChR2 stimulation before and after WIN application. Middle: WIN 55,212-2 effects on the IPSC amplitude mediated by SOM-INs and AM251 condition over time. WIN 55,212-2 effects in SOM-INs were significant after 30min of WIN application compared to AM251 condition, as tested by unpaired test ($p < 0.0001$) Right: Paired pulse ratio (PPR) in SOM-INs and AM251 condition before and after WIN application. Amplitude is normalized to 10 minutes of baseline for each single experiment. Bars indicate the standard error.

1.2.Evaluate the role of eCBs in Short-Term Depression (STD)

We confirm that SOM-INs are sensitive to the pharmacology activation of CB1R, however, we wondered whether endogenous cannabinoids release can activate CB1R from SOM-INs to modulate inhibitory response onto PNs. eCB-mediated STD is commonly triggered by depolarization of the postsynaptic cell, leading to a short-lived calcium dependent mobilization of eCBs and transient CB1R activation. This process is called depolarization-induced suppression of inhibition (DSI) or excitation (DSE) depending on the inhibitory or excitatory nature of the target synapse (Alger, 2002; Kano et al., 2009). To study STD, we patched PNs of layer 2/3 PFC at -65mV with a high chloride solution to record light- evoked IPSC from SOM-INs for 30 seconds of baseline. After baseline, we delivered a protocol of 5 second depolarizing steps, from -65mV to 0mV, to induce transient eCB release from PNs. After depolarization protocol, we back to -65mV to record light- evoked IPSC from SOM-INs for 80 seconds. In parallel experiments, we recorded light-evoked IPSC from PV-INs onto PNs to study whether eCBs induced by brief depolarization triggers STD. We found that brief depolarization triggers STD from SOM-INs (n=7) but not from PV-INs (n=8) (Figure 5). In addition, PPR were calculated in the light-evoked IPSC from SOM-INs and PV-INs before and after 5-second of depolarizing step. We found change in the light-evoked IPSC from SOM-INs (n=7, p= 0.0017, paired t-test), without changes in the light-evoked IPSC from PV-INs (n=4, p=0.1521, paired t-test). To calculate PPR, we used the same cells used in STD, however in the case of light-evoked IPSC from PV-INs, it was not possible to calculate PPR of all cells given the oversaturated IPSC in the second pulse (4 of 8 cells).

To corroborate whether STD from SOM-INs is mediated by CB1R activation through eCBs release, we did parallel experiments with 8uM of AM251 pre-incubation slices, and we delivered the same protocol used before in figure 5 (5 second of depolarizing step). We found that AM251

(n=8) prevents STD, confirming the involvement of CB1R in this form of plasticity (Figure 6). In PPR analysis, no changes were found in the AM251 condition compared to controls (SOM-Cre) (n=7, p=0.0906, paired t-test).

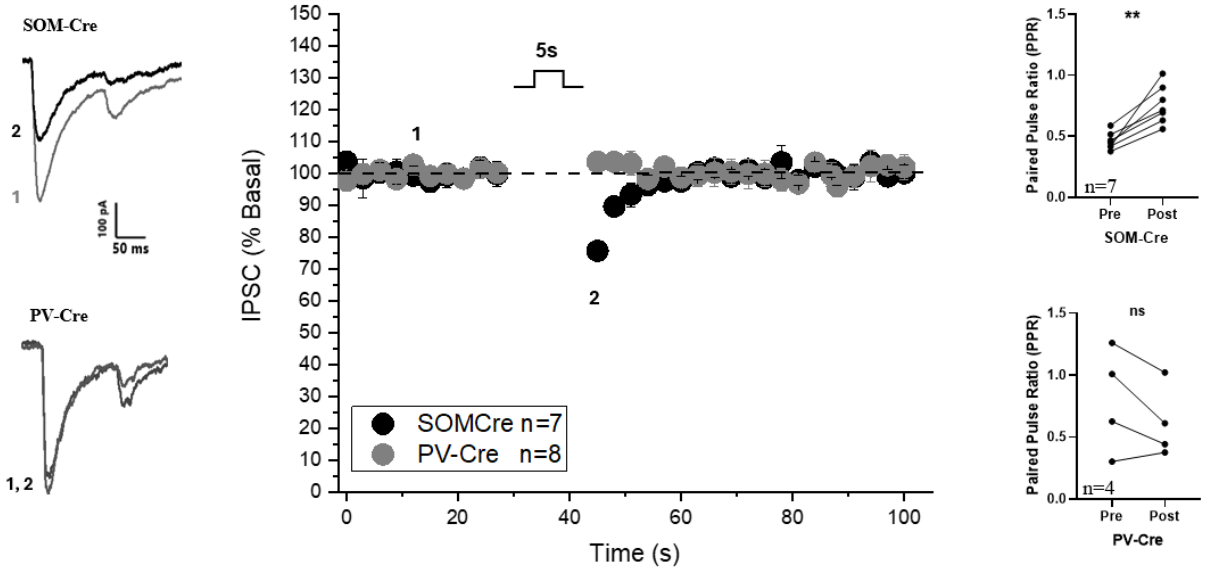

Figure 5. Brief depolarization triggers short-term plasticity from SOM-INs on pyramidal cells. Left: Representative traces of inhibitory response from SOM-INs and PV-INs on pyramidal cells using ChR2 stimulation before and after 5s of depolarizing step. Middle: 5s of depolarizing step effect on the IPSC amplitude mediated by SOM-INs and PV-INs over time. Right: Paired pulse ratio (PPR) in SOM-INs and PV-INs before and after 5s of depolarizing steps. Bars indicate standard errors.

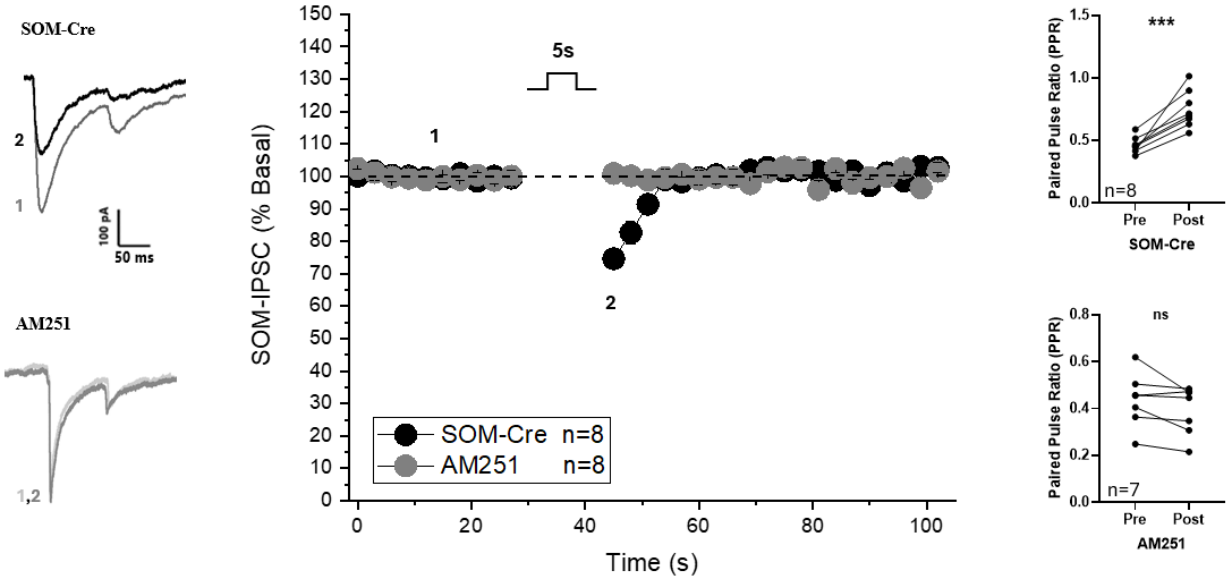

Figure 6. Short-term plasticity from SOM-INs is prevented by AM251 condition. Left: Representative traces of inhibitory response from SOM-INs and AM251 condition on pyramidal neurons using ChR2 stimulation before and after 5s of depolarizing step. Middle: 5s of depolarizing step effect on the IPSC amplitude mediated by SOM-INs and AM252 condition over time. Right: Paired pulse ratio (PPR) in SOM-INs and AM251 condition before and after 5s of depolarizing step. Bars indicate the standard error.

1.3.Evaluate the role of eCBs in Long-Term Depression (LTD)

In addition to STD, eCBs have shown to be involved in LTD of GABAergic inhibitory transmission. eCB-dependent LTD can be induced by an increase in neuronal activity, leading to an increase in calcium that results in the synthesis and release of eCBs from postsynaptic cells to bind presynaptic CB1 receptors. eCB-mediated plasticity requires glutamatergic afferent activity (Kreitzer & Malenka, 2005; Lafourcade et al., 2007; Michael C.Crair and Robert C.Malenka, 1995) and/or postsynaptic depolarization. To explore whether eCBs released by repetitive neuronal activity induce LTD from SOM-INs, we used a theta-burst stimulation (TBS) protocol, that

consists of stimulation of layer 1 (a train of five stimuli at 100 Hz x10) during postsynaptic depolarization of layer 2/3 PNs. First, we patched PNs of layer 2/3 PFC at -65mV with high chloride solution to record light-evoked IPSC from SOM-INs for 6 minutes of baseline. After baseline, PNs were depolarized from -65mV to +10mV, while we delivered the TBS protocol to induce eCB release. Cells were back to -65mV to record IPSC after TBS protocol for 30 minutes. In parallel experiments, we record light-evoked IPSC from PV-INs onto PNs to study whether eCBs release trigger by depolarization and TBS protocol induce LTD. We found that our protocol induces LTD in the light-evoked IPSC from SOM-INs without effect in the light-evoked IPSC from PV-INs, suggesting cell-type dependent effect (Figure 7). LTD were significant after 30 minutes of TBS protocol in the light-evoked IPSC from SOM-INs compared to light-evoked IPSC from PV-INs ($n=7$, $p<0.0001$, unpaired t-test). Interestingly, the same stimulation protocol resulted in inhibitory long-term potentiation (iLTP) from PV-INs. iLTP from PV-INs were significant after 30 minutes of TBS protocol compared to baseline ($n=6$, $p=0.0006$, paired t-test) (Figure 7). Changes in PPR analysis were found in the IPSC from SOM-Cre after TBS ($n=7$, $p= 0.0004$, paired t-test), and no change in the IPSC from PV-Cre ($n=6$, $p=0.3856$, paired t-test) (Figure 7). To corroborate whether LTD from SOM-INs is mediated by CB1R activation through eCBs release, we did parallel experiments adding 8uM of AM251 in pre-incubation slices for 15minutes. After pre-incubation, slices were put in the chamber recording to record light evoker-IPSC onto PN from SOM-INs. We depolarized PNs from -65mV to +10mV, while TBS protocol was delivered. We found that AM251 ($n=7$) prevents LTD from SOM-INs compared to control (IPSC from SOM-INs without AM251 condition) ($n=7$), confirming the involvement of CB1R in this form of plasticity (Figure 8). In the PPR analysis, no changes were found in the AM251 condition after

TBS protocol (n=7, p=0.9375, Wilcoxon test), compared to IPSC from SOM-INs (n=7, p=0.0054, paired t-test) (Figure 8).

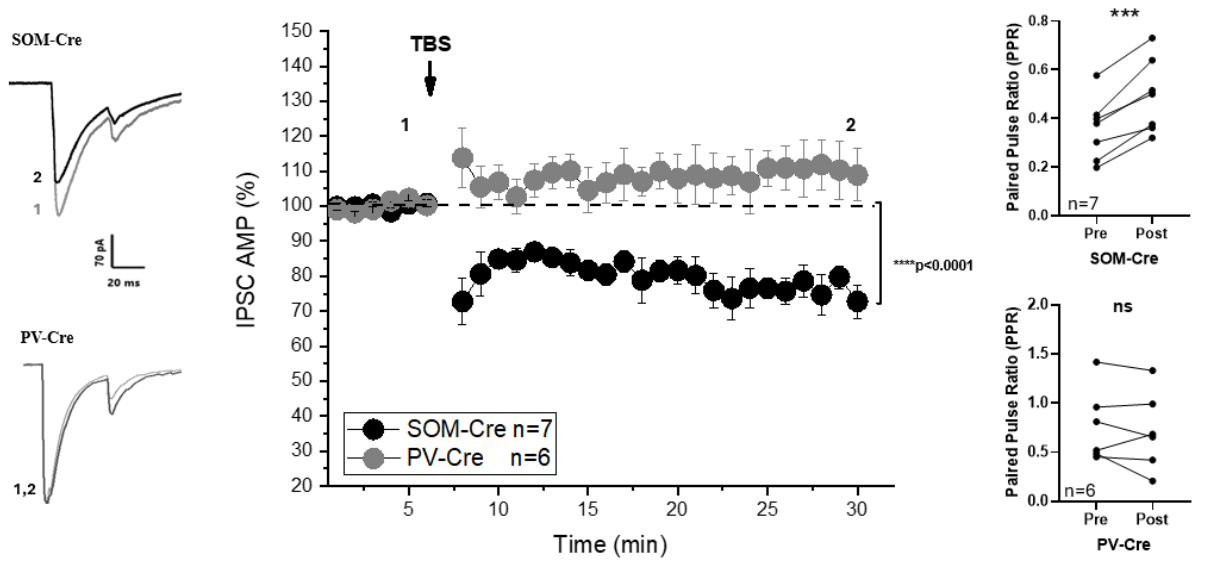

Figure 7. Theta Burst stimulation triggers long-term depression from SOM-INs. Left: Representative traces of light evoked-IPSC from SOM-Cre and PV-Cre (Gray): Middle: Theta-burst stimulation (TBS) in layer 1 triggers LTD of synaptic inhibition from SOM-INs but not from PV-INs. Right: Paired pulse ratio (PPR) in SOM-INs and PV-INs before and after TBS protocol. Significant differences were found in SOM-Cre compared to PV-Cre as tested by paired t-test. The amplitude was normalized to 6 minutes of baseline for each single experiment. Bars indicate the standard error.

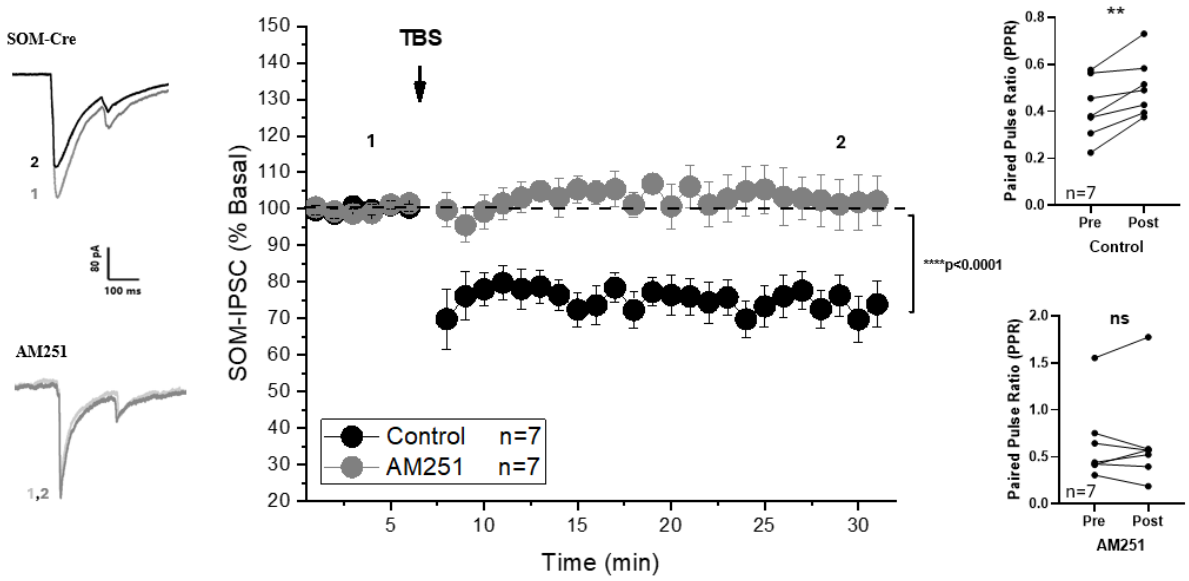

Figure 8. AM251 blocks long-term depression from SOM-INs. Left: Representative traces of light evoked-IPSC from SOM-Cre and AM-251 condition. Middle: Theta-burst stimulation (TBS) in layer 1 triggers long-term depression of synaptic inhibition from SOM-INs that is blocked by AM251. Right: Paired pulse ratio (PPR) in SOM-Cre and AM251 condition before and after TBS protocol. Significant differences were found in SOM-Crea, and no difference in AM251 condition as tested by paired t-test. The amplitude was normalized to 6 minutes of baseline for each single experiment. Bars indicate the standard error.

2. Investigate the cellular mechanism involved in synaptic plasticity mediate by eCBs

2.1. Evaluate the requirement of calcium and group 1 metabotropic glutamate receptors (I-mGluRs) in synaptic plasticity.

eCBs are retrograde messengers released from neurons by depolarization. This process involves intracellular Ca^{2+} concentration rise, by activation of group I metabotropic glutamate receptor (mGluR1 and mGluR5) and/or activation of Gq/11-coupled receptors (Ohno-Shosaku & Kano, 2014). To evaluate the cellular mechanism involved in iLTD from SOM-INs, we evaluate three possibilities that could participate in intracellular eCBs production. First, we

take advantage of the G protein inactivator, GDPβS. To this end, we patched PNs of layer 2/3 PFC at -65mV with high chloride solution to record light-evoked IPSC from SOM-INs for 6 minutes baseline. After baseline, PNs were depolarized from -65mV to +10mV, while TBS were delivered in layer 1 to induce eCB release from PNs. After TBS protocol, cells were back to -65mV to record light-evoked IPSC from SOM-INs, these recording were used as control group. In parallel experiments, we loaded the recording pipette with 1mM of GDPβS in the internal solution to patch and record light-evoked IPSC from SOM-INs by 6 minutes baseline. After baseline, we delivered TBS protocol to study whether eCBs can be produced and mediate iLTD from SOM-INs. We found that GDPβS blocked iLTD from SOM-INs after TBS protocol (Figure 9). Also, to study whether postsynaptic calcium is required for eCBS production, we loaded the recording pipette with 10mM of BAPTA, a calcium blocker, in the internal solution (high chloride) to patch PNs and to record light-evoked IPSC from SOM-INs at -65mV by 6 minutes of baseline. After baseline, we depolarize PNs from -65mV to +10mV while we delivered TBS protocol and recorded IPSC for 30 minutes. We found that BAPTA prevents iLTD from SOM-INs after TBS protocol (Figure 10). In addition, to study whether I-mGLUR are required for eCBs production, we take advantage of MCPG, an I-mGLUR antagonist. To this end, we added to the bath solution 100uM of MCPG, we patched PNs of layer 2/3 PFC at -65mV with high chloride solution to record light-evoked IPSC from SOM-INs for 6 minutes baseline. After baseline, PNs were depolarized from -65mV to +10mV while TBS were delivered in layer 1 to induce eCBs production from PNs. After TBS protocol, cells were back to -65mV to record light-evoked IPSC from SOM-INs for 30 minutes. We found that MCPG prevents iLTD from SOM-INs (Figure 10). LTD were significant after 30 minutes of TBS protocol in the light-evoked IPSC from SOM-INs in control (SOM-Cre) compared to light-

evoked IPSC in GDPβS, BAPTA and MCPG condition (n=6, p<0.0001, unpaired t-test). In addition, PPR analysis reveal no change of any drug condition after TBS protocol compared to controls (SOM-Cre) (GDPβS: n=7, p= 0.3750, Wilcoxon test; BAPTA: n=7, p= 0.7850, paired t-test; MCPG: n=7, p= 0.2085, paired t-test). Together, these results confirm that both calcium, activation of G-protein and I-mGLURs are required for iLTD-mediate eCB from SOM-INs.

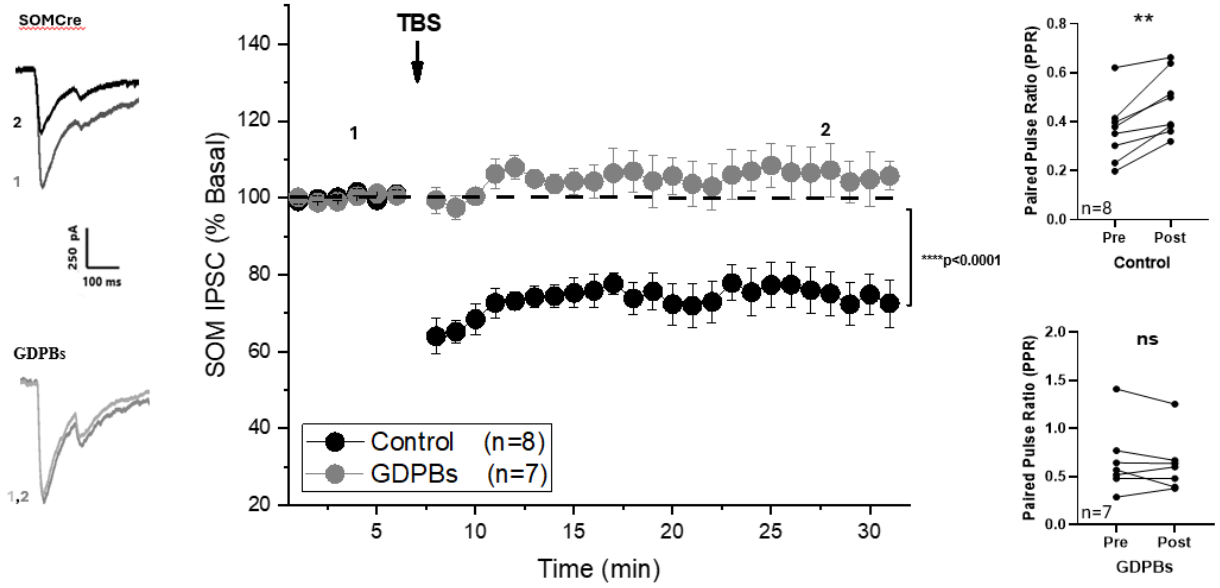

Figure 9. Long-Term depression from SOM-INs is blocked by the G protein inactivator GDPβS. Left: Representative traces of light evoked-IPSC from SOM-Cre and GDPβS condition. Middle: Theta-burst stimulation (TBS) in layer 1 trigger LTD of synaptic inhibition from SOM-INs that is blocked by GDPβS. Right: Paired pulse ratio (PPR) in control and GDPβS condition before and after TBS protocol. The amplitude was normalized to 6 minutes of baseline for each single experiment. Bars indicate the standard error.

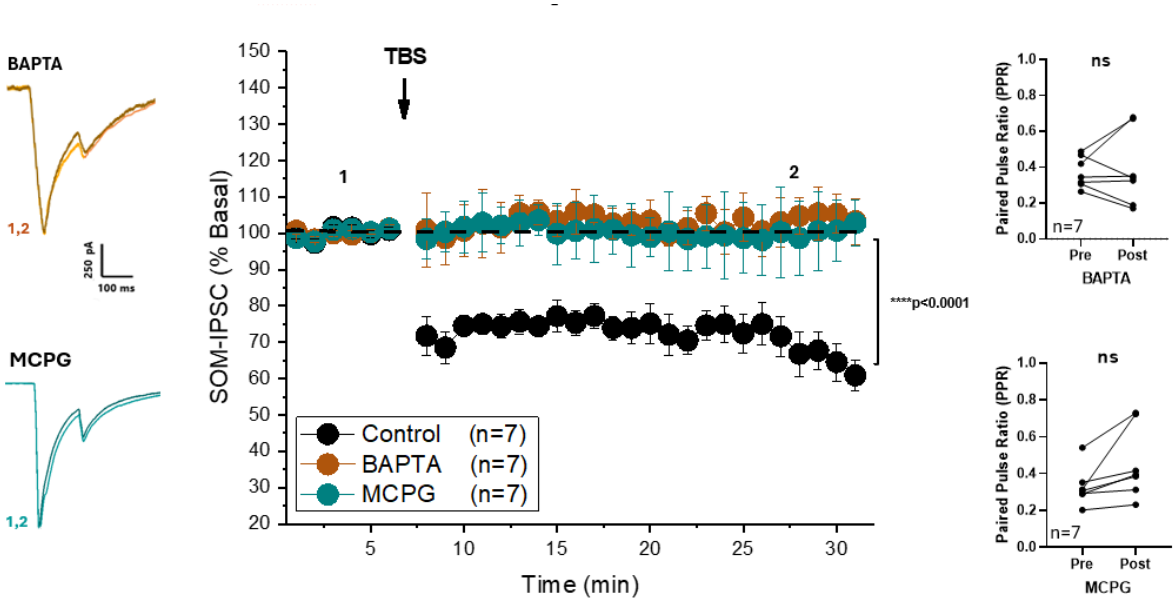

Figure 10. Long-Term depression requires intracellular Ca^{+2} and group I/II mGluRs. Left: Representative traces of light evoked-IPSC from SOM-INs, BAPTA and MCPG condition. Middle: TBS in layer 1 triggers LTD of synaptic inhibition from control, an effect that is blocked by BAPTA and MCPG. Right: Paired pulse ratio (PPR) in BAPTA and MCPG condition before and after TBS protocol. The amplitude was normalized to 6 minutes of baseline for each single experiment. Bars indicate the standard error.

2.2.Evaluate the role of neuromodulators in eCBs production.

It has been observed that eCB-LTD can also occur in response to activation of metabotropic receptors serotonin type 2 (5-HT2) GPCRs to stimulate DGL and lead to increased 2-AG production and calcium release from intracellular stores to participate in mobilizing eCBs (Maejima et al., 2001;Varma et al., 2001). To study whether 5-HT receptors are involved in eCBs production to mediate iLTD from SOM-INs, we used agonists and antagonists of 5-HTR to evaluate this possibility. To this end, we patched PNs of layer 2/3 PFC at +10mV with normal Cs^+ internal solution to record light-evoked IPSC from SOM-INs or PV-INs for 6 minutes baseline. After baseline, we transiently add 50uM of serotonin (5-HT) to the bath solution for 2 minutes, and we record light-evoked IPSC from SOM-INs or PV-INs for 30 minutes. We found that short bath application of 5-HT reduces the IPSC from SOM-INs, but not from PV-INs (Figure 11). Given that 5-HT acts through multiple receptors subtypes, including GPCRs (5-HT1A-B; 1D-F, 5-HT2A-C, 5-HT4, 5-HT5A, 5HT6 and 5-HT7) (Pytliak et al., 2011), we take advantage of TCB2, a specific 5-HT2 agonist, to study the specific implication of this receptor in eCBs production to mediate iLTD from SOM-INs. We patched PNs of layer 2/3 PFC at +10mV with normal Cs^+ internal solution to record light-evoked IPSC from SOM-INs or PV-INs for 6 minutes baseline. After baseline, we transiently add 10uM of TCB2 to the bath solution for 2 minutes, and we record light-evoked IPSC from SOM-INs or PV-INs for 30 minutes. We found that TCB2 also reduces inhibitory transmission from SOM-INs but not in PV-INS (Figure 12), suggesting the involvement of this subtype receptor in the inhibitory transmission from SOM-INs.

In addition, to study whether 5-HT2R is involved in eCBs release to mediate synaptic plasticity from SOM-INs, we used ritanserin, an antagonist of 5-HT2R. To this end, we added to the bath solution 4uM of ritanserin, we patched PNs of layer 2/3 PFC at -65mV with high chloride solution

to record light-evoked IPSC from SOM-INs for 6 minutes baseline. After baseline, PNs were depolarized from -65mV to +10mV while TBS were delivered in layer 1 to induce eCB production from PNs. After TBS protocol, cells were back to -65mV to record light-evoked IPSC from SOM-INs for 30 minutes. We found that ritanserin prevents iLTD from SOM-INs after TBS protocol (Figure 13). Together, these results suggest that 5-HT2R influence eCBs production that mediate synaptic plasticity from SOM-INs.

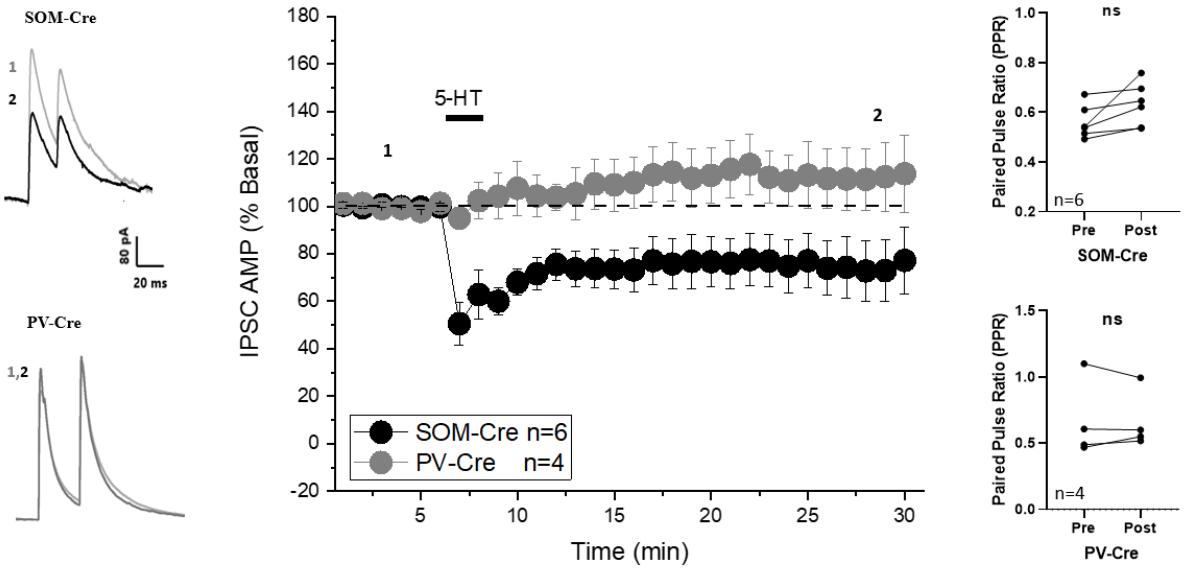

Figure 11. Serotonin decreases the amplitude of inhibitory response from SOM-INs. Left: Representative traces light evoked-IPSC from SOM-Cre and PV-INs. Middle: 5-HT effect on the IPSC amplitude mediate by SOM-INs and PV-INs onto pyramidal cells over time. Right: Paired pulse ratio (PPR) in SOM and PV-Cre before and after 5-HT application. The amplitude was normalized to 6 minutes of baseline for each single experiment. Bars indicate the standard error.

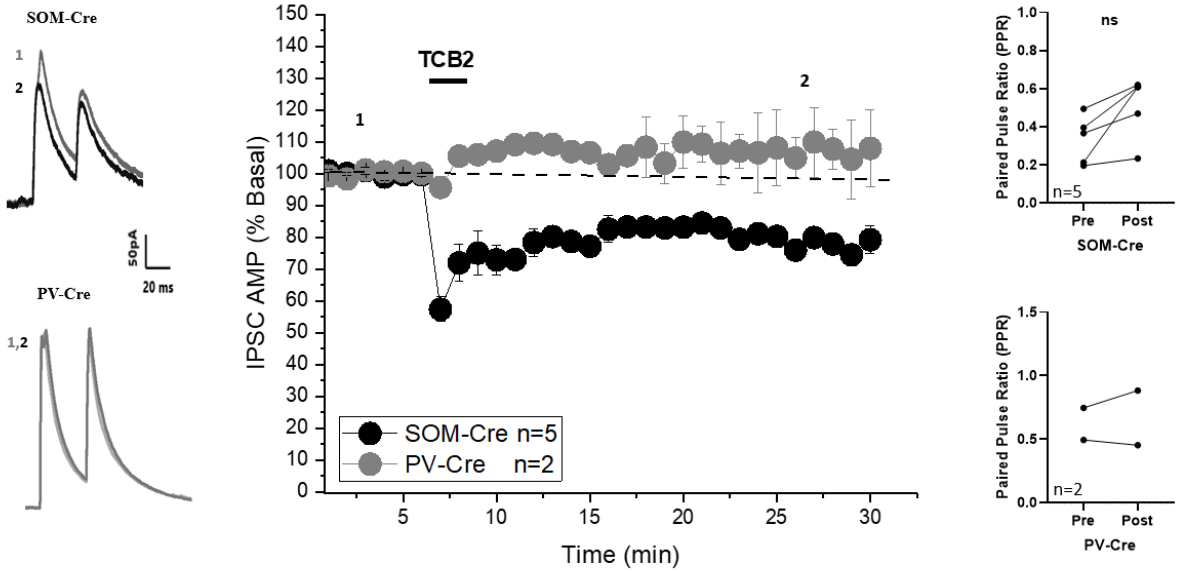

Figure 12. TCB2 decreases the amplitude of inhibitory response from SOM-INs. Left: Representative traces light evoked-IPSC from SOM-Cre and PV-Cre. Middle: TCB2 effect on the IPSC amplitude mediate by SOM-INs and PV-INs onto pyramidal cells over time. Right: Paired pulse ratio (PPR) in SOM and PV-INs before and after TCB2 application. The amplitude was normalized to 6 minutes of baseline for each single experiment. Bars indicate the standard error.

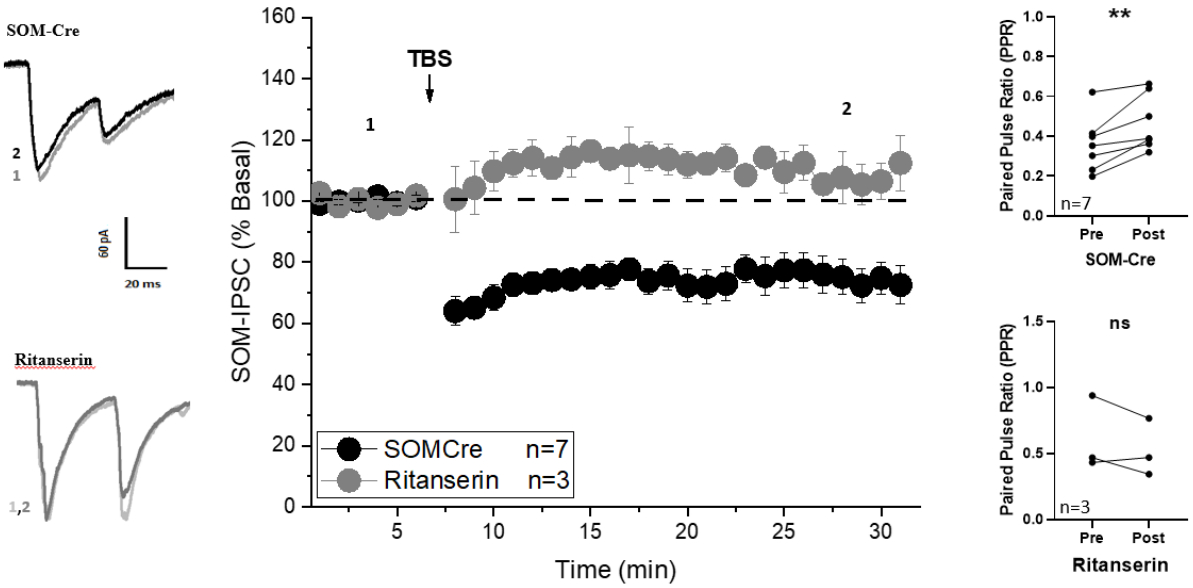

Figure 13. Ritanserin blocks long-term depression from SOM-INs. Left: Representative traces of light evoked-IPSC from SOM-Cre and in Ritanserin condition (Gray): Middle: Theta-burst stimulation (TBS) in layer 1 triggers long-term depression of synaptic inhibition from SOM-INs that is blocked by Ritanserin. Right: Paired pulse ratio (PPR) in SOM-Cre and Ritanserin condition before and after TBS protocol. The amplitude was normalized to 6 minutes of baseline for each single experiment. Bars indicate the standard error.

3. Investigate the consequence of CB1R loss from SOM-INs.

3.1.Confirm the absent of CB1R in SOM-INs by pharmacology drugs.

To study the impact of CB1R deletion in SOM-INs on synaptic transmission, we generated a transgenic mouse lacking CB1R expression in SOM-INs (SOM-Cre x floxed CB1). We used a genotype protocol that included DNA extraction, polymerase chain reaction (PCR) and gel electrophoresis to identify mice in which both alleles of cnr1, the gene encoding for CB1R, are floxed with at least one copy of the Cre recombinase (SOMCB1KO). We used WIN to pharmacologically activate CB1R and study the effect in the light evoked- IPSC from SOM-INs and SOMCB1KO mice. To this end, we patched clamp 2/3 PNs of PFC at +10mV with normal Cs^+ internal solution and we recorded light evoked-IPSC from SOM-Cre or SOMCB1KO for 6 minutes as baseline. After baseline, 5uM of WIN was added to the bath solution, and light evoked-IPSC were recorded for 30 minutes. We found the lack of WIN effect in SOMCB1KO compared to SOM-Cre (controls) (Figure 14). WIN effects were significant after 30 minutes in light evoked-IPSC from SOM-Cre compared to light evoked-IPSC from SOMCB1KO ($n=7$, $p<0.0001$, unpaired t-test). Interestingly, when we recorded basal transmission, we observed an increase in probability of release of GABA in SOMCB1KO mice evidenced by changes in PPR ($n=7$, $p= 0.0413$, unpaired t-test) (Figure 14). In addition to WIN, we also evaluate the effect of 5-HT and TCB2 on our transgenic mice. To achieve this, we patched PNs of layer 2/3 PFC at +10mV with normal Cs^+ internal solution to record light-evoked IPSC from SOM-INs or SOMCB1KO for 6 minutes baseline. After baseline, we add 50 uM of 5-HT or 10 uM of TCB2 to the bath solution for 2 minutes, and we record light-evoked IPSC from SOM-INs or SOMCB1KO mice for 30 minutes. We found that 5-HT and TCB2 reduce inhibitory transmission from SOM-INs but not in SOMCB1-KO (Figure 15,16), confirming the involvement of 5-HT2 and CB1R to mediate inhibitory transmission from SOM-INs.

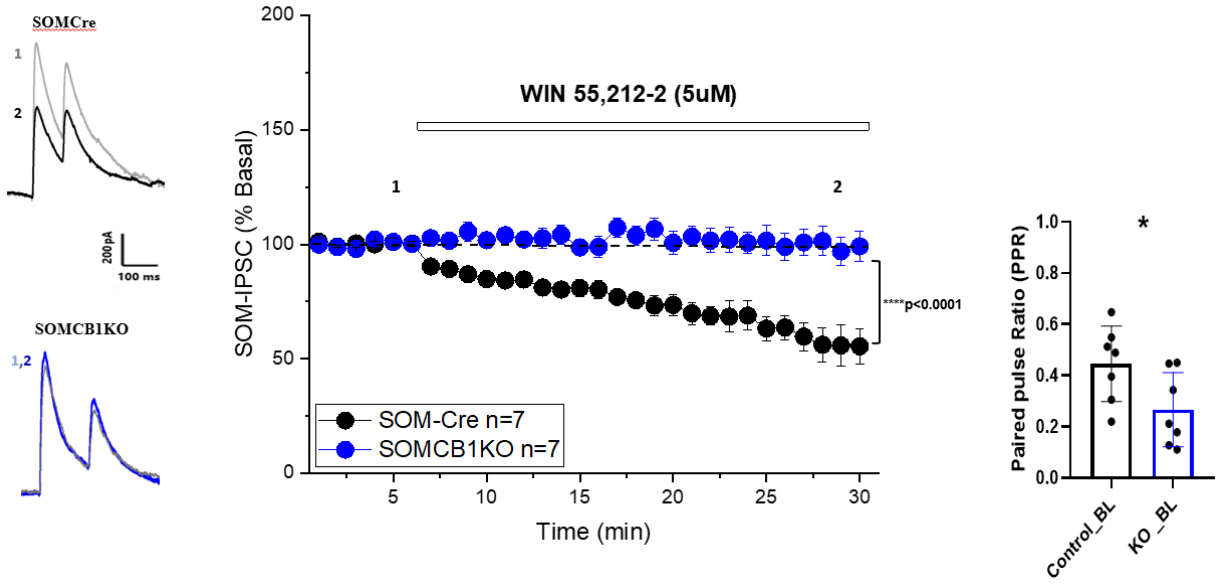

Figure 14. WIN 55,212-2 effect is absent in SOMCB1KO. Left: Representative traces of light evoked-IPSC before and after WIN application in the light evoked-IPSC from SOM-Cre and SOMCBIKO-INs. Middle: WIN effects on the IPSC amplitude mediated by SOM-INs and SOMCB1KO-INs onto pyramidal cells. Right: Paired pulse ratio (PPR) in SOM-INS and SOMCB1KO in basal transmission (*p<0.05). Amplitude is normalized to 6 minutes of baseline for each single experiment. Bars indicate standard errors.

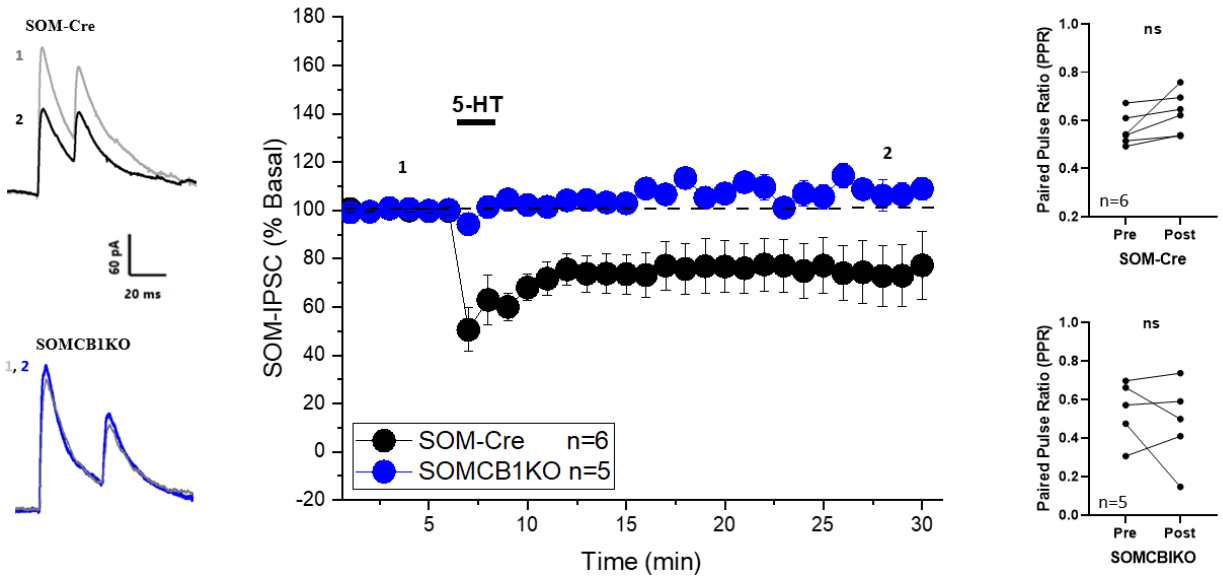

Figure 15. 5-HT effect is absent is absent in SOMCB1KO. Left: Representative traces of light evoked-IPSC before and after 5-HT application in SOM-Cre and SOMCBIKO-INs. Middle: WIN 55,212-2 effects on the IPSC amplitude mediated by SOM-INs and SOMCB1KO-INs onto pyramidal cells. Right: Paired pulse ratio (PPR) in SOM-INS and KO mice before and after 5-HT application. Amplitude is normalized to 6 minutes of baseline for each single experiment. Bars indicate standard errors.

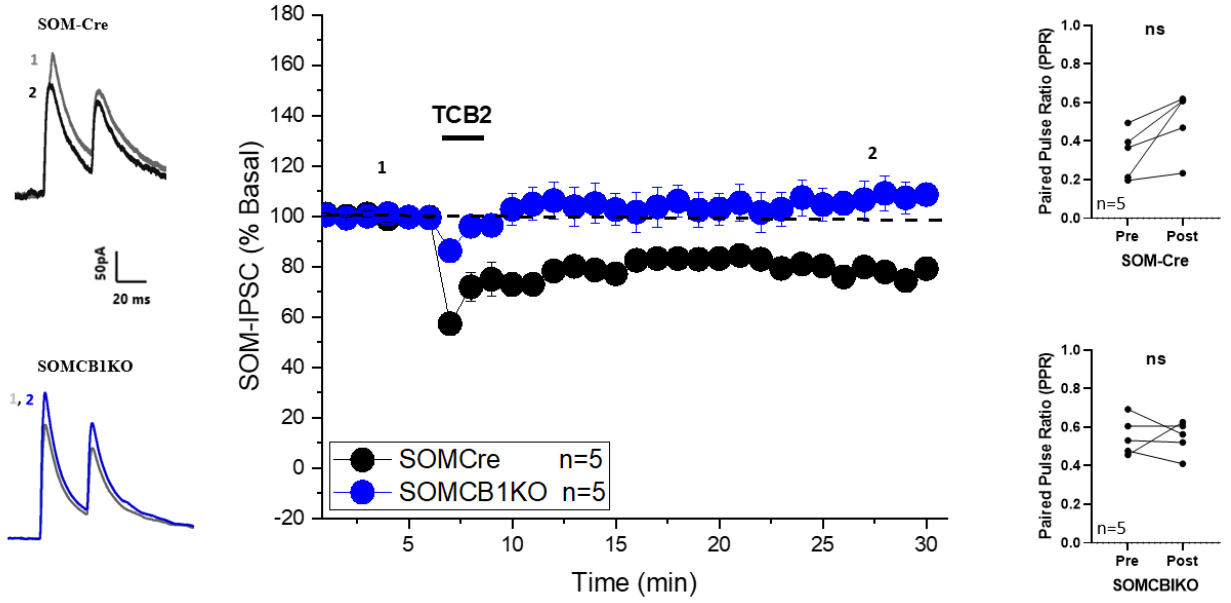

Figure 16. TCB2 effect is absent in SOMCB1KO. Left: Representative traces of light evoked-IPSC before and after TCB2 application in SOM-Cre and SOMCBIKO-INs. Middle: WIN 55,212-2 effects on the IPSC amplitude mediated by SOM-INs and SOMCB1KO-INs onto pyramidal cells. Right: Paired pulse ratio (PPR) in SOM-INS and KO mice before and after TCB2 application. Amplitude is normalized to 6 minutes of baseline for each single experiment. Bars indicate standard errors.

3.2.Evaluate the impact of SOMCB1KO in inhibitory and excitatory synapses.

We tested the impact of CB1 loss in STD and LTD from SOM-INs and SOMCB1KO mice. For STD experiments, we patched PNs of layer 2/3 PFC at -65mV with high chloride solution to record light- evoked IPSC from SOM-INs or SOMCB1KO for 30 seconds of baseline. After baseline, we delivered 5 second depolarizing steps, from -65mV to 0 mV, to induce transient eCBs release from PNs, and we back to -65mV to record light evoked-IPSC from SOM-INs or SOMCB1KO mice. We found that 5 second of depolarizing step induce transient depression of light evoked-IPSC from SOM-Cre but not in SOMCB1KO (Figure 17). For LTD experiments, we patched PNs of layer 2/3 PFC at -65mV with high chloride solution to record light-evoked IPSC from SOM-INs or SOMCB1KO for 6 minutes baseline. After baseline, PNs were depolarized from -65mV to +10mV, while we delivered the TBS protocol to induce eCB release from PNs. Cells were back to -65mV to record light evoked-IPSC from SOM-INs or SOMCB1KO after TBS protocol from 30 minutes. We found that TBS protocol induces LTD in the light evoked-IPSC from SOM-Cre but not from SOMCB1KO (Figure 18), confirming the involvement of CB1R to mediate synaptic plasticity from SOM-INs.

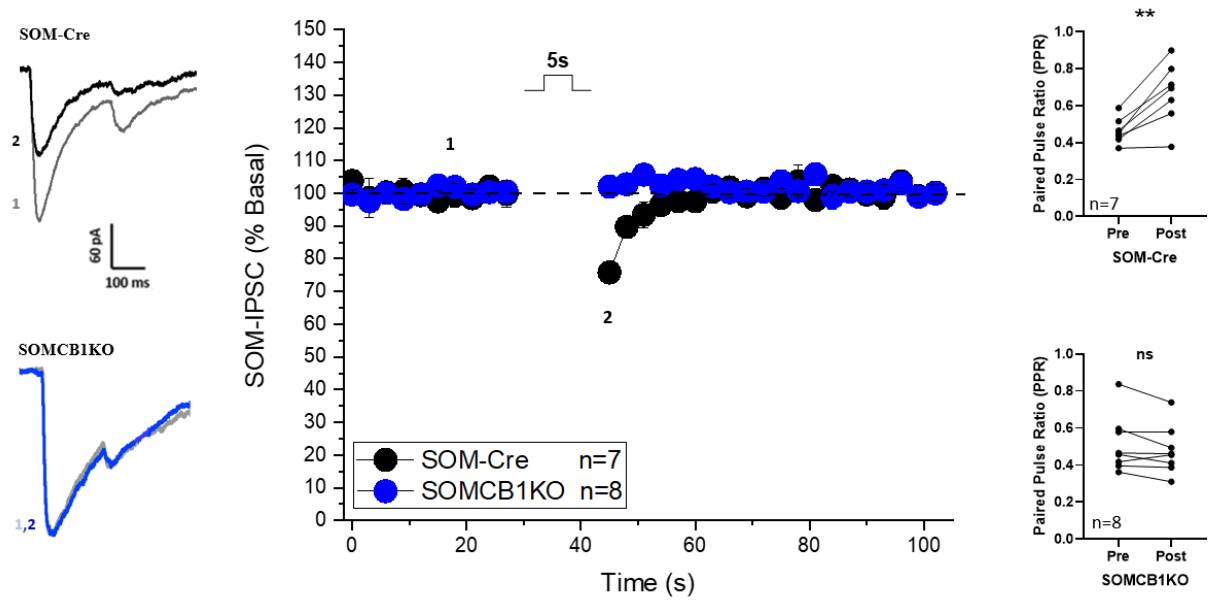

Figure 17. Short-term plasticity is absent in SOMCB1KO. Left: Representative traces of inhibitory response from SOM-Cre and SOMCBKO-INs onto pyramidal cells using ChR2 stimulation before and after 5s of depolarizing step. Middle: TBS effect on the IPSC amplitude mediated by SOM-Cre and SOMCB1KO-INs overtime. Right: Paired pulse ratio (PPR) in SOM-Cre and SOMCB1KO-INs before and after 5s of depolarizing step. Amplitude is normalized to 10 minutes of baseline for each single experiment. Bars indicate the standard error.

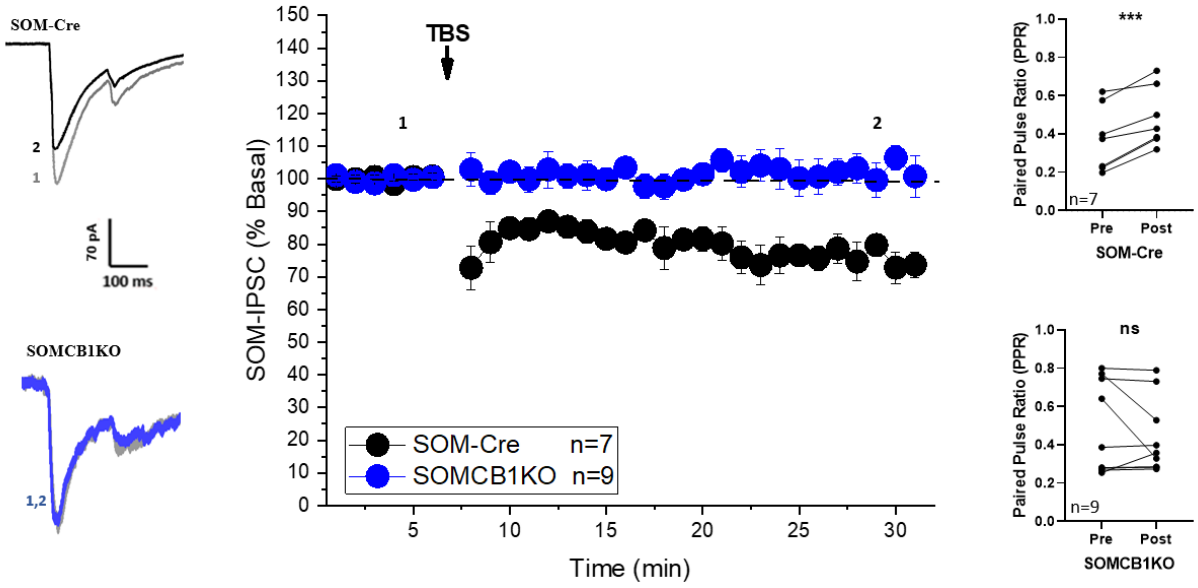

Figure 18. Long-term plasticity is absent in SOMCB1KO. Left: Representative traces of inhibitory response from SOM-Cre and SOMCBKO-INs onto pyramidal cells using ChR2 stimulation before and after Theta burst stimulation (TBS). Middle: TBS effect on the IPSC amplitude mediated by SOM-Cre and SOMCB1KO overtime. Right: Paired pulse ratio (PPR) in SOM-Cre and SOMCB1KO before and after 5s of depolarizing step. Amplitude is normalized to 6 minutes of baseline for each single experiment. Bars indicate the standard error.

We wondered whether our transgenic mice (SOMCB1KO) present changes, or alterations in inhibitory transmission. To achieve this, we electrically stimulated layer 1 of PFC with a monopolar electrode to deliver increased stimulus intensities (from 0V to 80V), and to recruit dendritic inhibition. We used SOMCB1KO as the experimental group and those that do not have Cre recombinase expression will serve as the control group (wild-type, WT). We patched layer 2/3 PNs of PFC at +10mV and we recorded the electrical evoked-IPSCs from SOMCB1KO and control mice to construct input-output (I-O) curves. We found that evoked dendritic inhibition was stronger in SOMCB1KO mice compared to controls, and significant differences were found at

high stimulus intensities (40V p=0.0087, 50V p=0.0416, 60V p=0.0035, 70V p=0.0010, 80V p<0.0001, one-way ANOVA, Sidak's multiple comparisons test) (Figure 19).

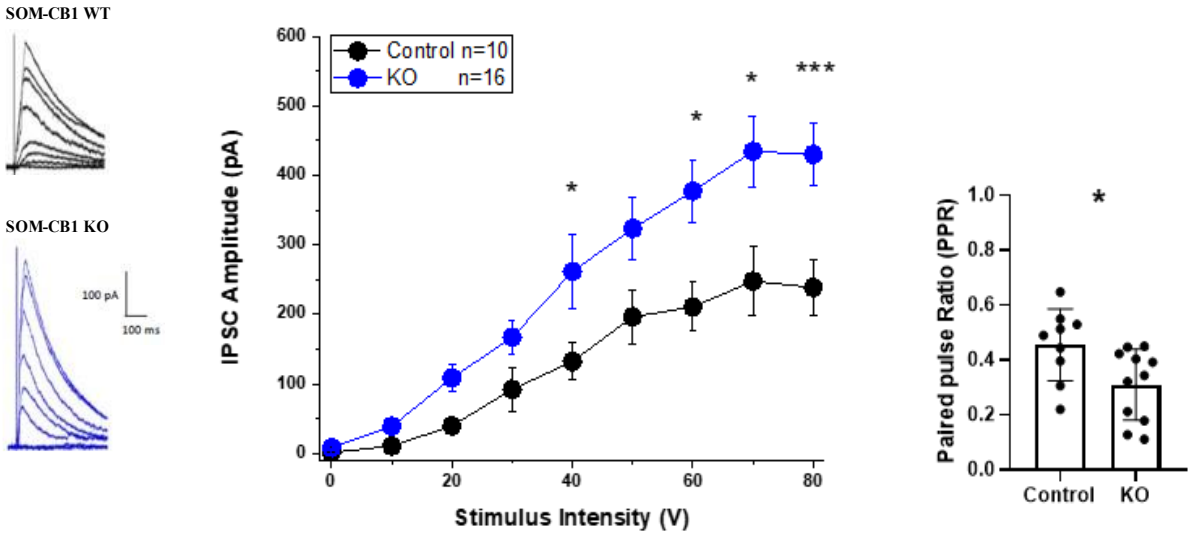

Figure 19. Input-Ouput curve of electric evoke-IPSC from SOMCB1WT and SOMCB1KO. Left: Representative traces of IPSC amplitude in SOM-CB1KO and SOM-CB1WT. Middle: Input-Output curve that represent summary plots of IPSCs responses to electrical stimulation between control and KO mice. Right: Paired pulse ratio for IPSCs between Control and KO mice collected with stimulation intensity at half max. Bars indicate the standard error.

In addition to studying the impact of CB1 deletion in SOM-INs onto inhibitory response, we tested basal inhibitory transmission in our SOMCB1KO mice. We patched 2/3 PNs of PFC at +10mV and we recorded the spontaneous IPSCs (sIPSC) activity by 2 minutes. We found an increase in sIPSC frequency in SOMCB1KO mice compared to controls (p=0.0369, unpaired test), with no change in sIPSC amplitude (p= 0.2940, unpaired test) (Figure 20). Therefore, according to the PPR

analysis, the probability of GABA release increases when CB1Rs are absent from the axon terminals of SOM-INs, which is consistent with greater inhibition in those animals. Together, these results evidence an enhancement of GABAergic synaptic transmission, that is also reflected in spontaneous inhibitory events in our transgenic mice (SOMCB1KO).

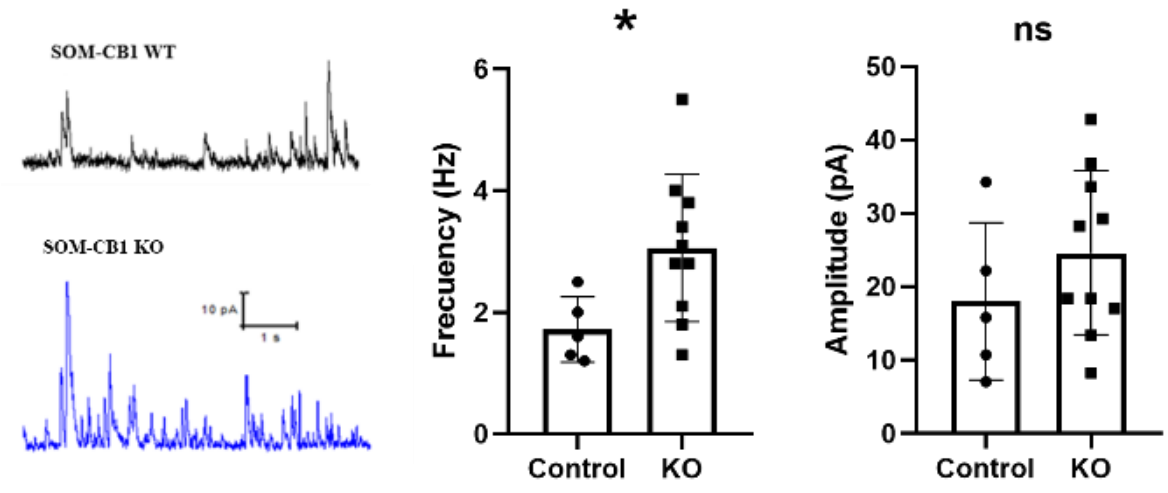

Figure 20. Spontaneous inhibitory activity in pyramidal neurons of layer 2/3 PFC. Left: Representative traces of spontaneous inhibitory response in SOM-CB1WT (controls) and SOM-CB1KO. Middle: Frequency of spontaneous inhibitory response in control and KO mice. Right: Amplitude of spontaneous inhibitory activity from controls and KO mice. Bars indicate the standard error.

In addition, to study the impact of CB1R loss on excitatory transmission, we electrically stimulated layer 1 of PFC with a monopolar electrode to deliver increased stimulus intensities (0V to 90V), while we patched and recorded at -65mV electrical evoked-EPSCs in layer 2/3 PNs of PFC to construct I-O curves in SOMCB1KO and control mice.

We found increased excitatory transmission at stimulation intensities ranging from 40V to 90V in SOM-CB1 KO mice compared to controls (40V $p=0.0146$, 50V $p=0.0001$, 60V $p<0.0001$, 70V $p<0.0001$; 80V<0.0001, 90V<0.0001, one-way ANOVA, Sidak's multiple comparisons test) (Figure 21). PPR analysis reveal changes in SOMCB1KO v/s control mice, suggesting presynaptic mechanisms (n=9, $p=0.117$, unpaired t-test). In addition, we recorded IPSC at +10mV and EPSC at -65mV at half stimulus intensity (40V) to measure E/I ratio in the same cell used to construct excitatory I-O curve (n=9). We found no change in SOMCB1KO and control mice (Figure 22) (n=9, $p=0.8260$, unpaired t-test). Moreover, we record spontaneous excitatory events. Notably, we found an increase in sEPSC frequency in SOM-CB1 KO mice compared to controls (n=9, $p=0.0016$, Mann Whitney test), without changes in sEPSC amplitude (n=9, $p=0.2814$, unpaired test) (Figure 23), suggested a presynaptic mechanism in excitatory transmission.

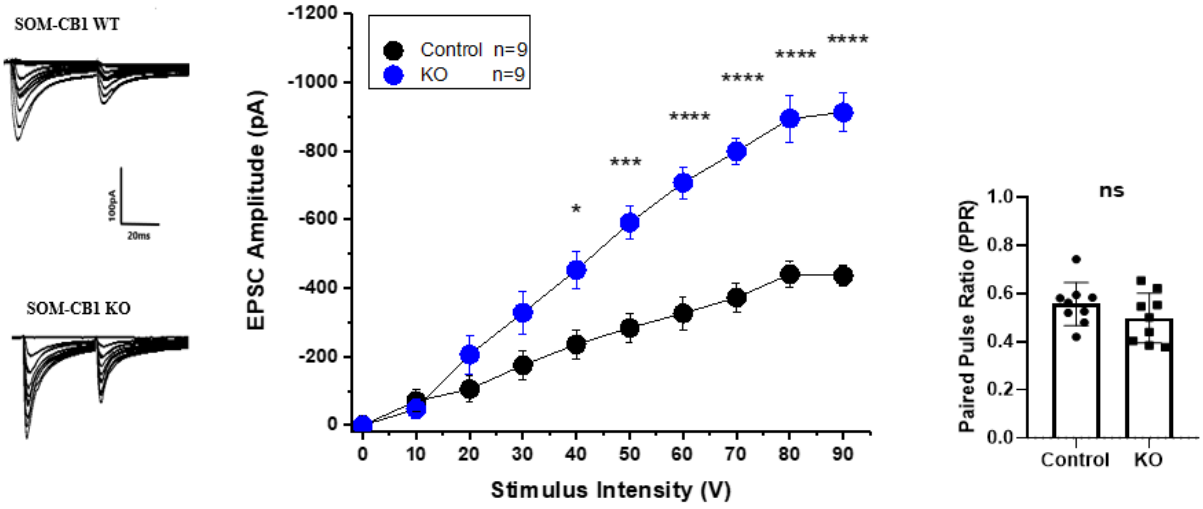

Figure 21. Input-Ouput curve of electric evoke-EPSC from SOMCB1WT and SOMCB1KO. Left: Representative traces of EPSC amplitude in SOM-CB1 KO and SOM-CB1 WT (controls) by increasing stimulus intensity (from 0V to 90V). Middle: Input-Output curve that represents summary plots of EPSCs responses to electrical stimulation between Controls and KO mice. Right: Paired pulse ratio between controls and KO mice at half max intensity. Bars indicate the standard error.

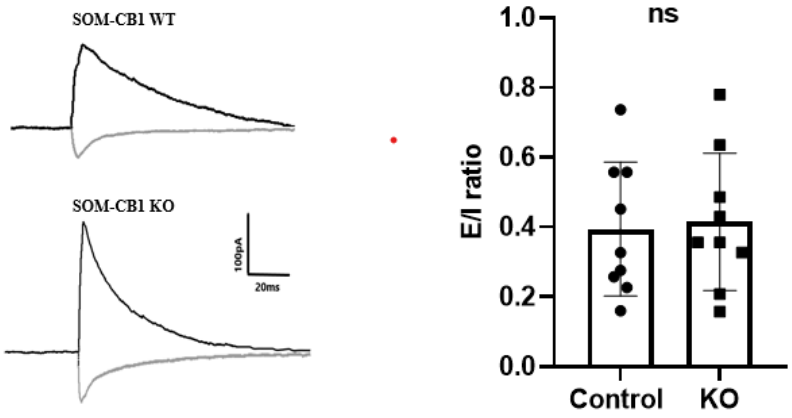

Figure 22. Excitation/Inhibition ratio between SOM-CB1WT and SOM-CB1KO. Left: Representative traces of electrical evoked-IPSC and EPSC from SOMCB1WT and SOMCB1KO collected at +10mV and -65mV respectively. Right: E/I ratio between SOM-CB1WT (controls) and KO mice calculated at half max intensity. Bars indicate the standard error.

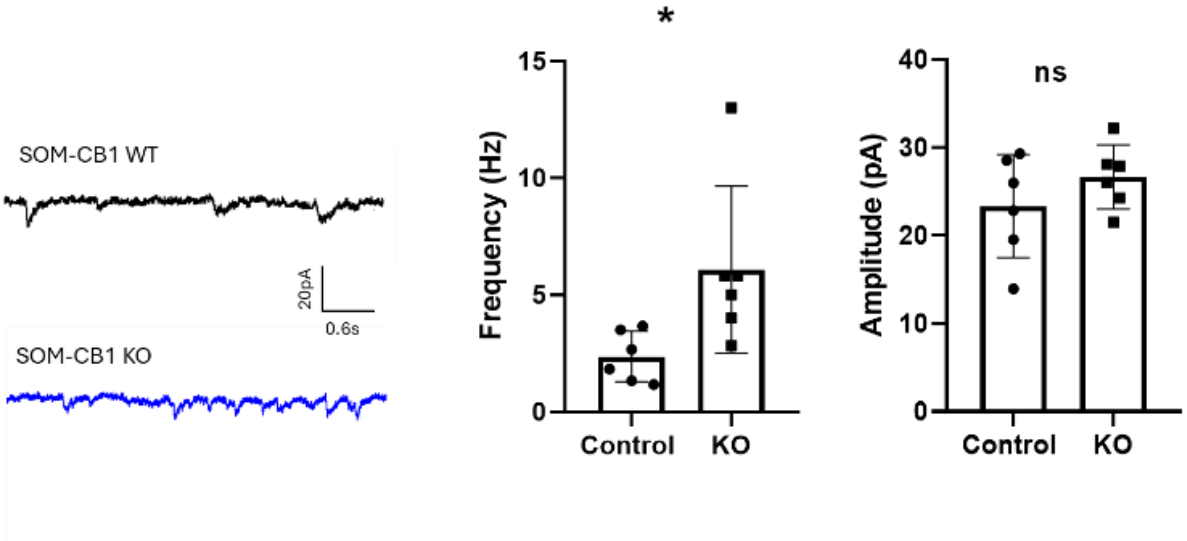

Figure 23. Spontaneous excitatory activity in pyramidal neurons of layer 2/3 PFC. Left: Representative traces of spontaneous excitatory response in SOM-CB1 WT and SOM-CB1 KO mice. Middle: Frequency of spontaneous excitatory activity in Control and KO mice. Right: Amplitude of spontaneous excitatory response in Control and KO mice. Bars indicate the standard error.

3.3.Evaluate synaptic changes and intrinsic properties in SOMCB1KO mice.

To test whether our transgenic mice have synaptic changes, we tested the ability to evoke action potential (APs) at different stimulus intensities in SOMCB1KO and SOM-CB1WT (controls). To this end, we electrically stimulated layer 1 of PFC with a monopolar electrode to deliver increased stimulus intensities (0V to 80V), while we recorded APs in PN of layer 2/3 PFC in the current clamp mode with a K^+ internal solution. We found that the threshold for inducing APs by synaptic excitation is decreased in SOMCB1KO (n=6, p=0.006, Mann Whitney test), as well as a lower half-intensity compared to controls (n=6, p= 0.0006, Mann Whitney test) (Figure 24).

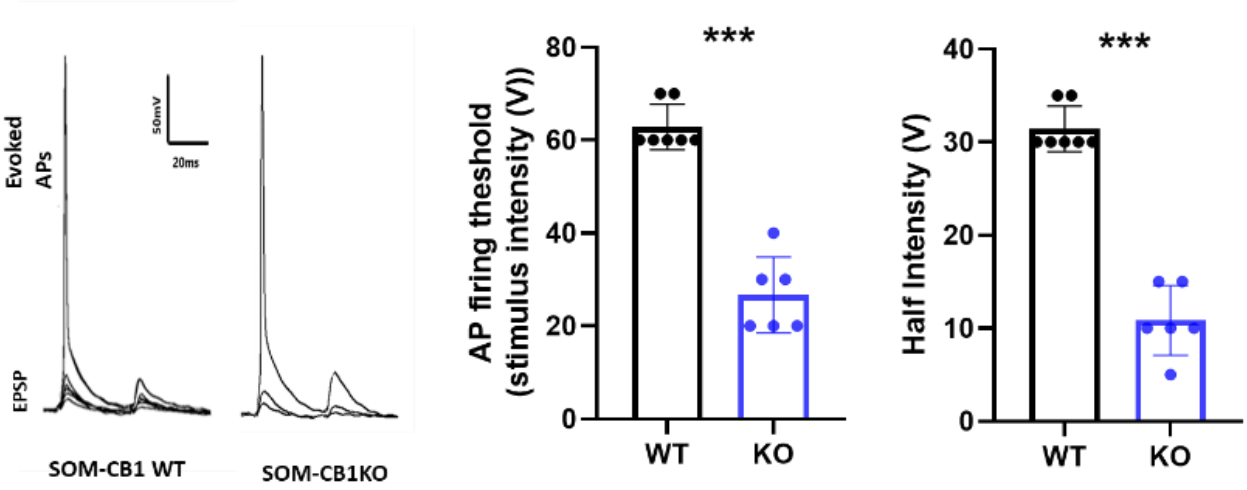

Figure 24. Probability to evoke action potential (APs) at 30V. Left: Representative traces of evoked AP in SOM-CB1 KO and SOM-CB1 WT after 5 pulses at 50Hz. Middle: Ratio of AP events by N° of pulses in WT and KO mice at 30V of stimulus intensity. Left: Half Intensity in WT versus KO.

As another way to evaluate synaptic changes, we investigated whether our KO mice have changes to temporarily add APs. First, we electrically stimulated layer 1 of PFC with a standard stimulus intensity (30V), while we deliver 5 pulses at 50Hz, and recorded APs in PN of layer 2/3 PFC in the current clamp mode with a K^+ internal solution. At 30V, SOMCB1KOs have a greater probability to generate APs in the first pulse compared to controls (SOM-CB1WT), which fire more frequently in the second pulse at that stimulus intensity ($p < 0.0001$, two-way ANOVA) (Figure 25). Given that the excitation is different between KO and WT cells, we analyzed the probability to evoke APs at the half-intensity for each cell. We found that KOs fire more frequently in the second pulse compared to WT ($p = 0.0009$, two-way ANOVA) (Figure 26).

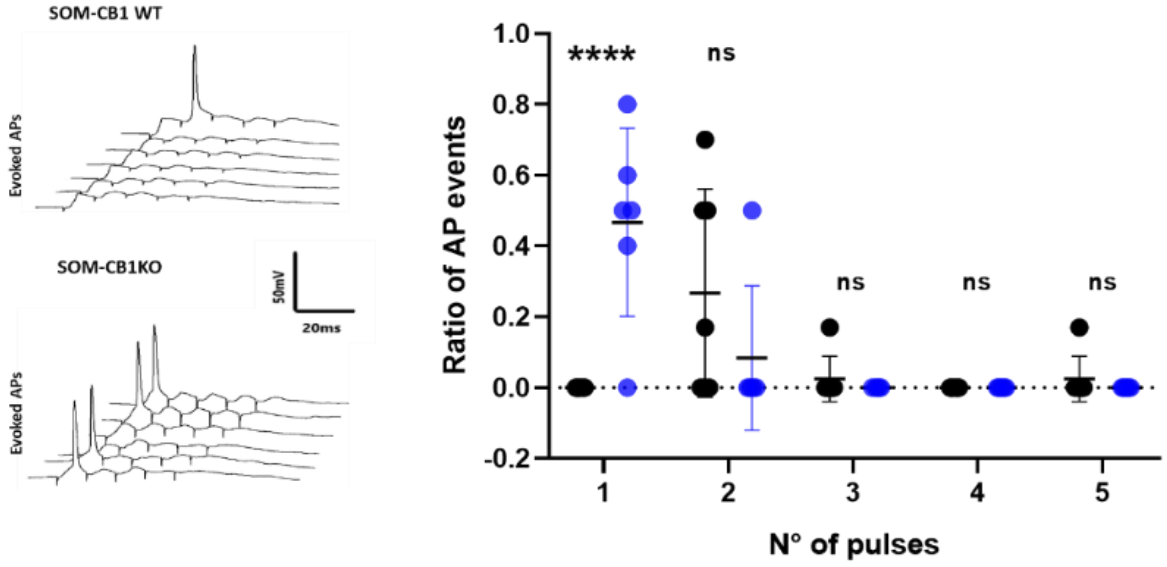

Figure 25. Probability to evoke action potential (APs) at half-maximal responses. Left: Representative traces of evoked AP in SOM-CB1 KO and SOM-CB1 WT after 5 pulses at 50Hz. Right: Ratio of AP events by N° of pulses in WT and KO mice at 30V of stimulus intensity.

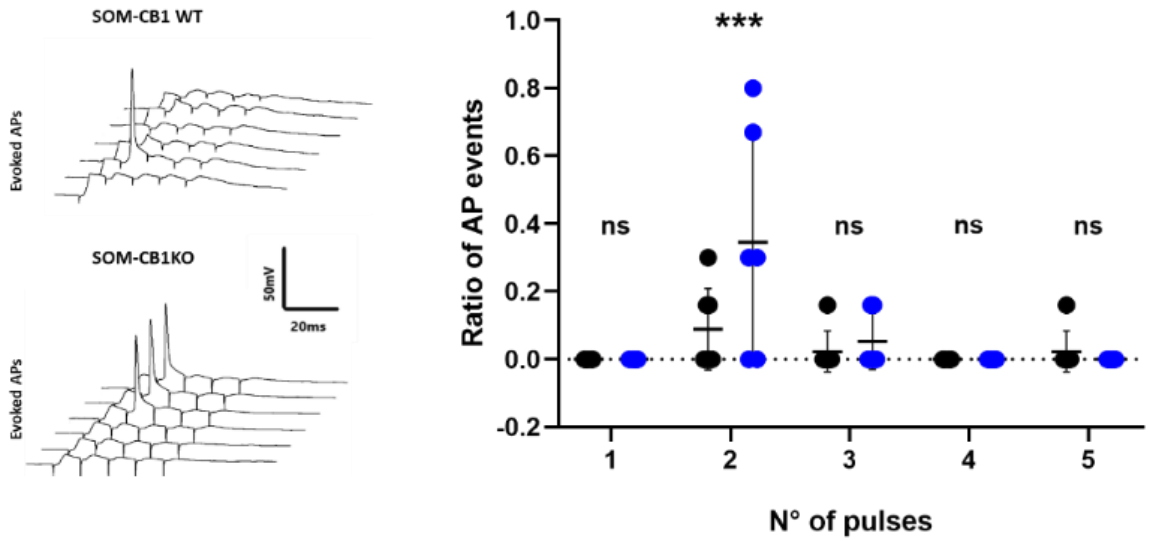

Figure 26. Probability to evoke action potential (APs) at the half-intensity for each cell. Left: Representative traces of evoked AP in SOM-CB1 KO and SOM-CB1 WT after 5 pulses at 50Hz. Right: Ratio of AP events by N° of pulses in WT and KO mice.

In addition, to study whether our results are consequences of change in intrinsic properties of INs, we patched SOMCB1KO-INs or SOMCB1WT-INs in current clamp mode with a K^+ internal solution. First, we injected SOMCB1KO-INs or SOMCB1WT-INs current step by 50pA from -300pA to +300pA to construct a voltage-current curve and study changes in the voltage membrane (Figure 26A-B). In addition, we made a ramp to inject positive current (from 0 to 200pA) to evoke action potential to calculate the membrane potential threshold through the derivative of voltage versus time to calculate the rheobase, which is the current at which the threshold is reached, as well as half-width and interevent-intervals. We did not find any changes in any of the following parameters: threshold membrane potential (Figure 26E: n=7, p= 0.8133, unpaired t-test), half-width (Figure 26F: n=7, p= 0.3383, unpaired t-test), rheobase (Figure 26G: n=7, p= 0.6102, unpaired t-test), interevent-intervals (Figure 26H: n=7, p= 0,7349, unpaired test).

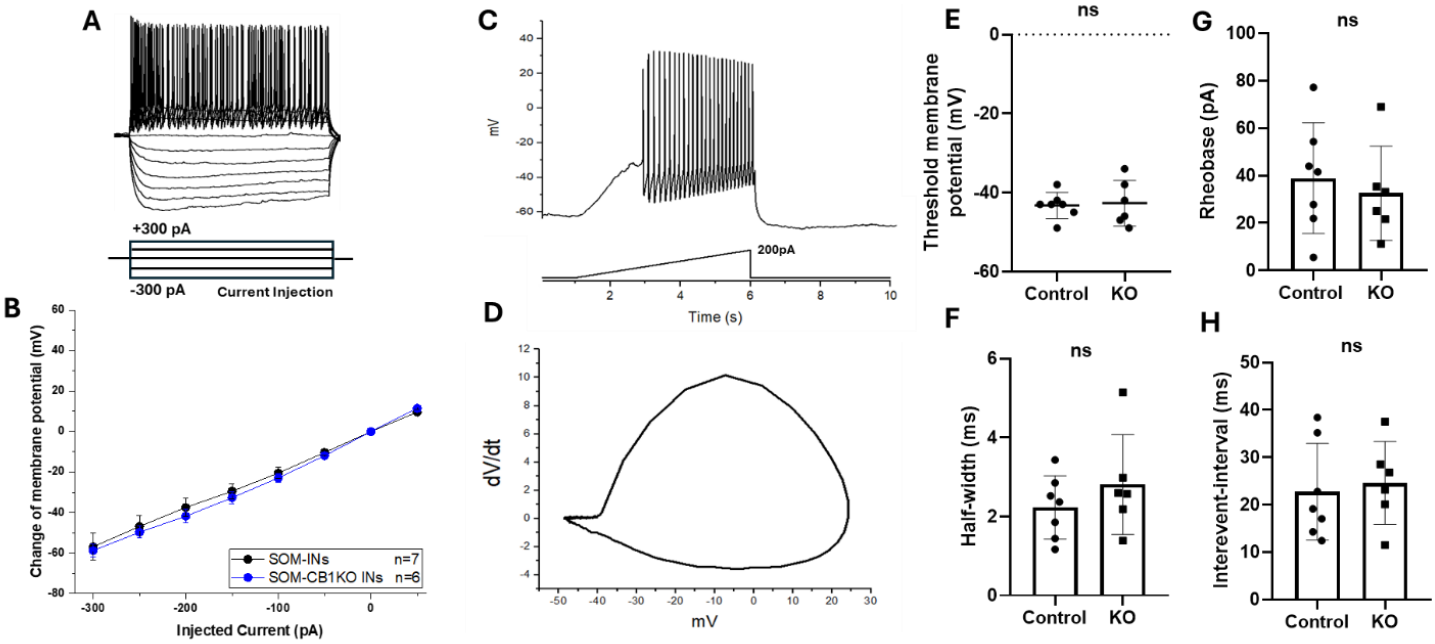

Figure 27. Intrinsic properties of SOM-CB1 WT and SOM-CB1 KO interneurons in layer 2/3 PFC. A: Representative scheme of current injection step from -300 to +300pA. B: Change of membrane potential (mV) between Control and KO interneurons. C: Representative scheme of positive current injections (from 0 to 200pA) to evoke action potential. D: Voltage versus time derivative. E: Threshold membrane potential in Control and KO interneurons. F: Half-width (ms). G: Rheobase (pA). H: Interevent-interval (ms).

DISCUSSION

In the neocortex, SOM-INs target the dendrites of postsynaptic glutamatergic PNs, forming synapses on both dendritic shafts and spines (Chiu et al., 2013). Through their inhibitory connections on dendritic arbors, SOM-INs modulate Ca^{2+} signaling, synaptic integration, and dendritic excitability. These dendritic inhibitory synapses are crucial for dendritic computation and can alter the integration of excitatory synaptic inputs (Chiu et al., 2013; Chiu et al., 2017).

The results of our study provide significant insights into the differential regulation of synaptic inhibition by CB1R activation in various INs subtypes within the PFC of the mammalian brain. CB1Rs are predominantly expressed in the axon CCK-INs, where their activation leads to suppression of GABA release. However, our study extends this understanding by exploring the role of CB1R in SOM-INs and PV-INs.

Role of CB1 receptors

eCBs play a crucial role in modulating neural activity in the brain by regulating both inhibitory and excitatory neurotransmission. Although CB1R are broadly distributed throughout the nervous system, the expression in the different types of INs and the role it plays is unknown. In the cortex and hippocampus, high levels of receptor expression are observed in CCK-INs, while PNs and PV-INs exhibit low or no expression, respectively (Kano et al., 2009). Given that in cortex, SOM-INs are the major subtype of INs, we explore the possibility that these INs are target for the action of eCBs.

It has been observed that CB1R activation can suppress GABA release onto layer 2/3 and 5 PNs of PFC(Chiu et al., 2010), thus, through its mechanism of action, retrograde eCBs signaling can significantly suppress GABA release from presynaptic terminals, leading to the disinhibition of PNs (Busquets-Garcia et al., 2018) in this brain area. SOM-INs target the dendrites of PNs

(Dumitriu et al., 2007;Chiu et al., 2013) to regulate the initiation of AP bursts generated via active currents in postsynaptic dendrites (Chiu et al., 2013). Therefore, regulation of eCBs through SOM-INs could potentially impact PNs activity in the PFC.

Our data demonstrates that WIN application, a CB1R agonist, selectively suppresses synaptic inhibition from SOM-INs but not from PV-INs onto PNs of layer 2/3 PFC in acute brain slices. This suppression of evoked-IPSCs from SOM-INs after 30 minutes of WIN application was 56.5 ± 14.49% compared to baseline, highlighting the role of CB1R in modulating the inhibitory inputs from SOM-INs. PPR ratio further supports these findings, revealing a significant change in SOM-INs after WIN application, suggesting presynaptic mechanism by which CB1R activation in SOM-INs modulates GABA release. Given that PV-IN are not sensitive to WIN application, we suggest specific roles of INs subtypes to modulate inhibition onto PNs that influence cortical circuitry, as well as a differential susceptibility to eCBs signaling.

To confirm the requirement of CB1R activation to suppress IPSCs from SOM-INs, we employed the selective CB1R blocker AM251, that abolished the effects of WIN on SOM-IPSCs. When we analyzed PPR, we observed significant difference after WIN application, which was absent in the presence of AM251. These results confirm the presynaptic role of CB1R in SOM-INs.

These findings have broad implications for our understanding of neural circuit regulation in the PFC. The selective modulation of SOM-INs by the CB1R suggests that eCB signaling can fine-tune inhibitory control in a subtype-specific manner, potentially influencing higher-order cognitive processes mediated by the PFC. The lack of effect on PV-INs highlights the functional specialization of INs subtypes and their unique contributions to cortical network dynamics.

Role of Endocannabinoids in Short-Term Depression (STD)

Our study aimed to elucidate the role of eCBs in STD of inhibitory synapses. We employed a 5-second depolarizing step protocol to induce transient eCB release from PNs, which mimics STD. Our findings indicate that brief depolarization selectively triggers STD from SOM-INs, but not from PV-INs. The significant change in PPR analysis observed in SOM-INs after depolarization supports this specific involvement of SOM-INs in eCB-mediated STD. In contrast, PV-INs did not exhibit such changes, suggesting that eCBs modulate inhibitory inputs from SOM-INs but not PV-INs. It is important to mention that not all pyramidal neurons exhibit the ability to produce and release eCBs under the same conditions. This variability can be attributed to many factors, including the differential expression of key enzymes required for eCB synthesis, as well as differences in intracellular signaling pathways and membrane properties. Some studies show that DAGL-α, which is essential for 2-AG production, is heterogeneously expressed across different brain regions and even within the same region across different neuronal subtypes, suggesting that certain PNs have reduced expression of the enzymes to synthesize eCBs, particularly 2-AG, the major retrograde eCB mediating STD like DSI and DSE. This variability is a key factor in determining which PNs can produce eCBs and influence synaptic transmission via retrograde signaling (Yoshida et al., 2006). In addition, it has been observed that not all PNs exhibit eCB-mediated suppression of GABAergic inhibition, suggesting that certain PNs may not produce or release sufficient eCBs to trigger retrograde signaling at inhibitory synapses (Bodor et al., 2005). The variability in this response was attributed to differences in the ability of PNs to synthesize and release eCBs, particularly 2-AG, in response to calcium influx. eCB synthesis is often dependent on calcium-dependent signaling pathways, and the activation threshold for these pathways can vary across neurons based on their intrinsic properties and prior activity levels. This means that eCB production and subsequent DSI induction are dependent on specific patterns of neuronal firing

and calcium dynamics, which may not be the same in all PNs (Lafourcade et al., 2007). In addition, PNs from different cortical layers and brain regions may exhibit distinct patterns of eCB production and release. For example, hippocampal CA1 PNs have demonstrated robust eCB signaling and DSI, whereas PNs in the PFC exhibit comparatively less eCB-mediated synaptic modulation (Neu et al., 2007). This suggests a region-specific difference in the ability of PNs to produce eCBs and modulate synaptic transmission. Interestingly, within the vHPC-PFC circuit, CCK-INs that target intratelencephalic (IT) cells in the PFC do show eCB modulation through DSI, while pyramidal tract (PT) cells do not (Liu et al., 2020). Together, these findings highlight both regional and cell-type-specific differences in eCB signaling, suggesting that eCB modulation is finely tuned depending on both the brain region and the specific neural circuit involved. Tonic eCB release can differentially affect PNs and INs depending on their location, leading to variations in DSI across different brain regions, including the hippocampus and cortex (Freund & Katona, 2007). Also, prolonged or basal eCB signaling can lead to receptor desensitization, thereby influencing the likelihood of observing DSI at certain synapses (Monory et al., 2006). Therefore, tonic eCB signaling can desensitize CB1Rs, making them less responsive to eCBs released during DSI-inducing stimuli, and this variability could account for why DSI is observed in some PNs or SOM-IN synapses but not others (Kim & Alger, 2010). Here we showed that SOM-INs are sensitive to short-term eCBs release, however we do not know which subtypes of SOM-INs are responsible for the response we observed, given that CB1 receptor expression differs across SOM-IN subtypes. For example, while Martinotti cells in the cortex are known to be involved in providing distal dendritic inhibition, only a subset of these cells expresses CB1Rs. These CB1R-expressing Martinotti cells are involved in eCB-mediated synaptic modulation via DSI (Bodor et al., 2005)

When we use the selective CB1R blocker AM251, we confirmed the role of CB1R in this type of plasticity. AM251 prevented the occurrence of STD from SOM-INs, as evidenced by the absence of significant changes in PPR analysis under AM251 treatment. These results underscore the importance of CB1R in mediating STD specifically from SOM-INs, highlighting the subtype-specific nature of endogenous cannabinoid release and signaling in cortical circuits.

Role of Endocannabinoids in Long-Term Depression (LTD)

Our investigation also extended to the role of eCBs in LTD from GABAergic inhibitory transmission. Using TBS protocol to induce eCBs, we demonstrated that eCB-dependent LTD can be induced from SOM-INs but not from PV-INs. The significant changes in PPR analysis in SOM-Cre following TBS, and the lack of changes in PV-Cre further support the cell-type specific nature of this plasticity. The blocking effect of AM251 on LTD in SOM-INs, confirmed by unchanged PPR values, suggests a presynaptic mechanism mediated by CB1R activation.

eCBs are released from postsynaptic neurons in response to calcium influx or G-protein-coupled receptor (GPCR) activation, binding to CB1 receptors on presynaptic terminals. This binding inhibits GABA release by reducing presynaptic calcium influx and disrupting the neurotransmitter release machinery. When this process persists over extended periods, it leads to iLTD, characterized by a sustained decrease in GABAergic inhibitory transmission. This form of synaptic plasticity enables postsynaptic neurons to dynamically regulate inhibitory input, often as a homeostatic response to shifts in excitatory activity. Our findings indicate that SOM-INs are particularly sensitive to eCB-mediated inhibition of GABA release, supporting the notion that, in the PFC, CB1 receptors are expressed on SOM-IN terminals, in addition to their established expression on CCK-INs. These results indicate that eCBs play a crucial role in modulating long-term inhibitory synapses by regulating GABA release through CB1 receptors located on the

presynaptic terminals of SOM-INs. Their influence on inhibitory synapses underpins various forms of synaptic plasticity, including iLTD. However, the extent and effectiveness of eCB-mediated modulation of GABA release can vary depending on multiple factors. One critical factor is the density and distribution of CB1 receptors, which could differ among various GABAergic INs subtypes, including SOM-INs and CCK-INs. The sensibility of presynaptic terminal to eCBs can vary based on factors such as intracellular calcium buffering, the state of CB1R phosphorylation, or the availability of other regulatory proteins that modulate CB1R signaling (Chevaleyre et al., 2007). Moreover, differences in the presynaptic machinery that governs vesicle release can lead to differential responses to eCB-mediated suppression of GABA release at different subtypes of INs. Additionally, the availability of eCBs, such as anandamide and 2-AG, are tightly regulated by their synthesis and degradation via enzymes like diacylglycerol lipase (DAGL), fatty acid amid hydrolase (FAAH), and monoacylglycerol lipase (MAGL), which can influence the strength and duration of eCB signaling. Postsynaptic neurons synthesize eCBs on demand, but the amount of eCBs produced can vary depending on the strength of synaptic activity, calcium levels, and activation of GPCRs. Different neurons may produce varying levels of eCBs in response to similar stimuli, leading to variability in the degree of GABA release suppression (Heifets & Castillo, 2009). The variability in GABA release suppression due to eCB signaling allows for fine-tuning of inhibitory tone in different neural circuits. For instance, in some cases, the reduction of GABA release can enable increased excitatory input, facilitating processes like long-term potentiation (LTP). In this context, our results demonstrate a robust induction of iLTD from SOM-INs following TBS protocol, which is consistent with eCB-mediated plasticity mechanisms. Interestingly, the same stimulation protocol resulted in inhibitory long-term potentiation (iLTP) from PV-INs (n=6, p=0.0006, paired t-test), suggesting a differential role of

eCB signaling across INs subtypes. This iLTP from PV-INs could reflect a compensatory mechanism aimed at preserving the E/I balance by increasing GABA release, potentially due to homeostatic plasticity mechanisms. It is possible that eCB production selectively targets SOM-INs, reducing their inhibitory influence, while PV-INs, which express fewer CB1 receptors, experience an upregulation of synaptic strength to counteract the diminished inhibition from SOM-INs. This dynamic interplay between SOM and PV-INs could be crucial for maintaining network stability and cognitive functions in regions such as PFC. To further explore the compensatory mechanism observed in PV-INs following TBS and its potential link to eCB signaling, more experiments will be needed to provide deeper mechanistic insights (Udakis et al., 2020).

eCB-mediated iLTD often requires the activation of Gq/11-coupled metabotropic receptors, such as group I metabotropic glutamate receptors (I mGluRs), muscarinic M1/M3 acetylcholine receptors, and serotonin 5-HT2 receptors. These receptors play a pivotal role in initiating intracellular signaling cascades that drive the synthesis and release of eCBs, particularly 2-AG, through the phospholipase C (PLC) β–diacylglycerol lipase (DGL) pathway. To further explore the cellular mechanisms driving eCB-mediated synaptic plasticity, we investigated the roles of intracellular calcium and group I mGluRs. The application of the G-protein inactivator GDPβS effectively blocked LTD following TBS protocol, underscoring the critical requirement for Gq/11-coupled receptor activation in this form of plasticity. These findings highlight the intricate interplay between Gq/11-coupled receptors, including muscarinic, serotonin, and glutamate receptors, and intracellular signaling pathways, such as calcium dynamics, in mediating eCB-dependent synaptic plasticity. However, variability in the expression levels of these Gq/11-coupled receptors, or their coupling efficiency to downstream eCB-producing enzymes, can result in differential magnitudes of iLTD (Marsicano & Lutz, 1999). For example, in certain synapses, mGluR signaling may be

more prominent, leading to enhanced eCB production and a more robust suppression of inhibitory transmission.

Additionally, the calcium chelator BAPTA prevented iLTD, demonstrating the essential role of intracellular calcium signaling in triggering eCB production. The blockade of iLTD by the group I mGluR antagonist MCPG further confirmed the requirement of this receptor activation for this process. Activation of mGluR1 and mGluR5 is known to trigger the production of eCBs, particularly 2-AG, which serves as a retrograde messenger that modulates presynaptic neurotransmitter release via CB1 receptors (Castillo et al., 2012). This crosstalk enables a highly regulated form of synaptic modulation, where mGluR activation, coupled with an intracellular Ca^{2+} rise, leads to local production of eCBs, orchestrating LTD at specific synapses.

The absence of significant changes in PPR analysis in any drug condition indicates that these interventions specifically disrupt the eCB-mediated signaling pathway rather than alter presynaptic mechanism. These results highlight the significance of eCBs signaling in mediating LTD in PFC, a mechanism that has also been observed in other brain regions, as has previously described (Chevaleyre & Castillo, 2003; Gerdeman et al., 2002; Safo & Regehr, 2005; Marsicano et al., 2002).

Serotonin role in Modulating Inhibitory Transmission

Serotonin (5-HT) is an important modulatory neurotransmitter in the brain that plays a role in both normal physiology and pathologies such as migraine, depression, fear and anxiety, obsessive compulsive disorders, schizophrenia, and addiction (Gray & Roth, 2007). 5-HT modulates synaptic transmission by binding to various 5-HT receptor subtypes, which are G-protein-coupled receptors (GPCRs). 5-HT2 receptors, such as 5-HT2A, and 5-HT2C, are coupled to the Gq/11

signaling pathway, activating PLC, wich catalyzes the production of diacylglycerol (DAG), a key precursor for 2-AG synthesis (Best & Regehr, 2008).

Our data reveals that short-term application of 5-HT reduces inhibitory transmission from SOM-INs over time but does not affect inhibitory transmission from PV-INs. This selective reduction in inhibitory transmission from SOM-INs suggests a specific interaction between 5-HT signaling and eCBs production in these INs. In addition, the application of TCB2, a 5-HT2 receptor agonist, similarly reduced inhibitory transmission from SOM-INs, indicating that 5-HT2 subtype receptors are involved in this process. We also observed that blocking 5-HT2 receptors with ritanserin disrupted this signaling pathway, preventing the production of eCB release and in this way, suppressing iLTD from SOM-INs. These results suggest a crosstalk between 5-HT2 and CB1 receptors, where 5-HT2 receptor activation is necessary for triggering the eCB system that mediates iLTD in SOM-INs. Therefore, without 5-HT2 activation, the cascade for eCB-mediated synaptic plasticity is interrupted. This selective modulation of inhibitory transmission from SOM-INs by 5-HT2 receptor activation highlights the complex regulatory mechanisms underlying eCB production and function. The involvement of neuromodulators like 5-HT in eCB-mediated plasticity suggests that neurotransmitter systems can influence synaptic plasticity through intricate signaling pathways. The influence of 5HT to promote eCBs release to activate CB1 receptors may provide a mechanism for fine-tuning inhibitory control in cortical circuits, potentially impacting various cognitive and emotional processes.

We observed that MCPG prevents eCB-mediated iLTD from SOM-INs. Without mGluR activation, the retrograde signaling of eCBs to bind presynaptic CB1 receptors is disrupted, a mechanism essential for reducing GABA release at inhibitory synapses. Many forms of iLTD, especially those observed in hippocampal and cortical INs, are initiated by mGluR-dependent

mechanisms, where glutamate release and subsequent mGluR activation trigger the necessary eCB signaling for long-term plasticity. Thus, activation of mGluRs and 5HT2 are critical steps in iLTD mediated by eCBs. However, more experiments will be necessary to study the contribution of other 5-HT receptors to the neural inhibitory circuits. In addition, future research should aim to delineate the molecular pathways through which 5-HT2 receptor activation leads to eCB production and synaptic plasticity in SOM-INs. Investigating the role of other neuromodulators in eCB signaling could provide a broader understanding of how different neurotransmitter systems interact to regulate synaptic function. Additionally, exploring the behavioral consequences of disrupting 5-HT2 and CB1 receptor interaction could offer insights into the role of this crosstalk in neuropsychiatric disorders. Understanding these interactions is essential for developing targeted therapeutic strategies for disorders characterized by dysregulated synaptic plasticity at inhibitory synapses.

Role of CB1R in Synaptic Transmission and Plasticity

It is known that deletion or pharmacological blockade of CB1Rs on GABA INs disrupt eCB-mediated plasticity in many brain regions (Albayram et al., 2015) and genetic deletion of CB1R from GABAergic neurons (GABA/CB1$^{-/-}$) leads to behavioral changes such as enhanced interest to social stimuli (Terzian et al., 2014) and enhanced neuroinflammation in aging (Albayram et al., 2015) as well as hyperphagia (Bellocchio et al., 2010) and developmental deficits (Díaz-alonso et al., 2012). Pharmacological studies reveal that the cannabinoid system regulates the development of the GABAergic system. For example, exposure to the CB1R agonist WIN during adolescence impairs brain maturation and prenatal WIN treatment alters migration of GABAergic neurons in the cortex (Cass et al., 2014;Saez et al., 2014). Exogenous activation of CB1Rs on GABAergic INs disrupts hippocampal-dependent learning in vivo (Puighermanal et al., 2009) and inhibits LTD of excitatory synapses in the amygdala in vitro (Azad et al., 2008). In this context, given the effect

in brain function when CB1Rs are disrupted, we studied and explored the role of CB1R in synaptic transmission and plasticity by generating transgenic mice lacking CB1R expression specifically in SOM-INs. The absence of CB1R in SOM-INs provided a unique opportunity to investigate the specific contributions of CB1R to inhibitory and excitatory synaptic transmission. Our findings showed that WIN agonist did not affect SOMCB1KO INs, suggesting successful deletion of CB1R. Basal transmission analysis revealed an increased probability of GABA release in SOMCB1KO mice, as evidenced by changes in PPR. This suggests that CB1R normally acts to suppress GABA release from SOM-INs. Additionally, the application of 5-HT and TCB2, a 5-HT2 receptor agonist, reduced inhibitory transmission from SOM-INs in control mice but not from SOMCB1KO-INs, confirming the lack of effect when we remove CB1R from SOM-INs, an effect that is absent even when we stimulate 5-HT2R to trigger eCBs release.

We also investigated the impact of CB1R deletion on synaptic plasticity by evaluating both STD and LTD from SOM-INs. In control mice, a 5-second depolarizing step induced DSI, whereas no such effect was observed in SOMCB1KO. Similarly, TBS induced iLTD from SOM-INs but not from SOMCB1KO-INs, confirming the essential role of CB1R in mediating synaptic plasticity from SOM-INs.

Impact of CB1R deletion on Inhibitory Synaptic Transmission

By removing CB1Rs selectively from SOM-INs, we were also able to assess the impact of this loss on inhibitory synaptic transmission. Given that electrical stimulation recruits GABAergic synapses from different sources, we placed a monopolar electrode in layer 1 of PFC to focally recruit dendritic inhibition and to enhance the contribution of inhibitory transmission from SOM-INs onto layer 2/3 PN. We found that dendritic inhibition evoked in layer 1 was stronger in the SOMCB1KO mice compared to controls (SOMCB1WT), with significant differences found at

increased stimulation intensities in the I-O curve. This increase in inhibition was consistent with changes in PPR analysis and an increase in sIPSC frequency, suggesting an enhanced probability of GABA release in the absence of CB1Rs on SOM-INs axon terminals. These results highlight the importance of CB1Rs at SOM-INs where a dys-regulation of the eCB system may contribute to developing several neuropsychiatric diseases that are characterized by inhibitory hyperactivity. In some studies, the optical silencing of SOM-INs resulted in a greater decrease in the frequency of spontaneous IPSCs in striatal spiny projection neurons (SPNs) in a Huntington disease (HD) model, suggesting that SOM-expressing INs are the main contributors to the overall increased GABA synaptic activity in HD SPNs (Holley et al., 2019).

Impact of CB1R deletion on Excitatory Synaptic Transmission

Information processing requires temporally and spatially coordinated synaptic communication, which constitutes a balance between excitatory and inhibitory cells (E/I ratio) and is implicated in neuropsychiatric disorders such as schizophrenia. Our result shows that CB1R deletion increases GABA inhibition mediated by SOM-INs. In addition to inhibitory transmission, we also evaluated the impact of CB1R loss on excitatory synaptic transmission by constructing I-O curves for evoked excitatory postsynaptic currents (EPSCs). We observed increased excitatory transmission at increased stimulation intensities in SOMCB1KO mice compared to controls. Changes in PPR analysis and spontaneous excitatory events (sEPSCs) further supported an enhancement in excitatory transmission, suggesting a presynaptic mechanism. However, no change in E/I ratio was observed, supporting a homeostatic effect on SOMCB1KO mice, where an increase in inhibition was compensated by an increase in excitation. Neural circuit functions involve finely controlled excitation/inhibition interactions that allow complex neuronal computations. In that context, it has been observed that during sensory processing in neocortex, presentation of a sensory stimulus can recruit inhibition in addition to excitation, leaving the excitation/inhibition balance unperturbed

(Gabernet et al., 2005; Xue et al., 2014;Letzkus et al., 2015), an effect that could be important to ensure temporally precise firing or even to create a brief window of opportunity for firing, However, given that CB1 receptors are involved in fine-tuning synaptic plasticity at inhibitory synapses, their absence could result in hyperactivation of SOM-INs, leading to greater GABA release, but without the necessary coordination between inhibitory and excitatory inputs. This disruption in synaptic plasticity could account for the increase in both IPSCs and EPSCs. The circuit may attempt to compensate for the lack of CB1-mediated inhibition, which could explain the simultaneous increase in inhibitory and excitatory drive. In this sense, more experiments will be needed to corroborate nature or source of increased excitation in SOMCB1KO.

Impact of CB1 Receptor Loss in Network Excitation

SOM-INs, typically slow-spiking, provide delayed and sustained inhibition targeting the distal dendrites of PN, thus allowing an initial window of excitatory input. In SOMCB1KO mice, the absence of CB1-mediated modulation could further alter the timing of GABA release, potentially prolonging this window for excitation. PV-INs, that often provide faster inhibition, arrive earlier and control perisomatic synaptic input. The loss of CB1 receptors on SOM-INs would affect the late-phase, dendritic inhibition, thus shifting the excitatory-inhibitory balance towards excitation during the early phase of synaptic responses (Lovett-Barron et al., 2012; Pouille et al., 2009). Considering this possibility, we measured the ability to evoke action potentials (APs) in response to varying stimulus intensities in SOMCB1KO and control mice. Our results demonstrated that SOMCB1KO mice exhibited a lower threshold for AP induction and an increased probability of generating APs at lower stimulus intensities compared to controls. This suggests a heightened excitation in the absence of CB1 receptors on SOM-INs, which may reflect alterations in the E/I balance. Furthermore, SOMCB1KO mice showed an increased probability of generating APs on the first pulse of a standard stimulus intensity, indicating enhanced synaptic responsiveness or

reduced inhibitory tone compared to wild-type (WT) mice. These findings suggest that the removal of CB1-mediated inhibition from SOM INs leads to a shift in network excitation, which is consistent with previous reports on the role of CB1 receptors in regulating cortical inhibitory circuits (Hill et al., 2007; Marsicano & Lutz, 1999).

CB1 receptors typically reduce the probability of neurotransmitter release, including GABA. In absence of CB1 receptors in SOMCB1KO mice, GABA release may become less regulated or increased in terms of frequency, but without the precise activity-dependent modulation that CB1 receptors provide. This loss of timing precision may impair the synchrony between excitation and inhibition, potentially opening a temporal window for excitatory input, in circuits where SOM-INs play a key role in shaping dendritic integration (Katona & Freund, 2012).

Intrinsic Properties

Despite the observed alterations in synaptic transmission and neuronal excitability, our analysis revealed no significant differences in the intrinsic properties between SOMCB1KO and control mice. Electrophysiological parameters such as resting membrane potential, action potential half-width, interevent intervals, rheobase, and threshold membrane potential remain unchanged, suggesting that the observed changes in synaptic function and excitability are specifically due to the loss of CB1 receptors in SOM-INs rather than inherent alterations in their cellular properties. These findings indicate that CB1R deletion selectively affects network level excitability and synaptic plasticity without fundamentally altering the baseline characteristics of SOM-INs, highlighting the role of CB1R signaling in modulating E/I balance while preserving intrinsic neuronal function. However, further investigations are warranted to explore potential compensatory mechanisms and circuit-level adaptations. These studies could incorporate calcium imaging in SOM-INs to provide dynamic insights into intracellular signaling changes that may

accompany the observed electrophysiological results. Additionally, assessing CB1R deletion effects on other INs subtypes beyond SOM and PV-INs, such as vasoactive intestinal peptide (VIP)-expressing interneurons, could reveal broader circuit-wide impacts and potential interneuron crosstalk.

Furthermore, in vivo electrophysiological recordings under behavioral paradigms will be critical to determine how these cellular and synaptic changes translate into functional outcomes, such as cognitive, sensory processing, and anxiety-related behaviors. Integrating these approaches will provide a more comprehensive understanding of the role of CB1R in shaping inhibitory networks and their contributions to overall brain function.

Future directions

Future studies should explore the underlying molecular mechanisms that confer CB1R sensitivity to SOM-INs but not PV-INs and other subtypes of INs. The differential sensitivity of SOM-INs and PV-INs to eCB signaling suggests distinct functional roles for these INs in cortical circuits. This subtype-specific regulation has significant implications for the development of targeted therapies for neurological and psychiatric disorders characterized by dysregulated eCB signaling and inhibitory neurotransmission.

Additionally, investigating the behavioral and cognitive consequences of selective CB1R modulation and the selective deletion of CB1R in SOM-INs could provide valuable insights into the role of eCB signaling in health and disease.

In conclusion, our study elucidates a critical role for CB1R in regulating synaptic inhibition from SOM-INs in the PFC, contributing to the broader understanding of eCB signaling and its impact on cortical circuitry. CB1R plays a crucial role in regulating synaptic transmission and plasticity in SOM-INs. The deletion of CB1R leads to increased GABA release probability, enhanced

inhibitory and excitatory transmission, and greater synaptic excitability without altering intrinsic neuronal properties. These findings highlight the importance of CB1R in maintaining synaptic balance and plasticity within cortical circuits, with potential implications for understanding the role of eCB signaling in neurological disorders. Further research is needed to explore the behavioral consequences of these synaptic alterations and their relevance to cortical circuits.

ACKNOWLEDGMENTS

This work was funded by grants from the chilean national research and development agency (ANID) to Nicole Sanguinetti (PhD fellowship 21202528), and Chiayu Chiu (regular Fondecyt 1171840).

BIBLIOGRAFY

Albayram, Ö., Passlick, S., Bilkei-gorzo, A., Zimmer, A., & Steinhäuser, C. (2015). Physiological impact of CB1 receptor expression by hippocampal GABAergic interneurons. *Pflugers Arch*, *468*(4), 727–737. https://doi.org/10.1007/s00424-015-1782-5

Alger, B. E. (2002). *Retrograde signaling in the regulation of synaptic transmission : focus on endocannabinoids* (Vol. 68).

Araque, A., Castillo, P. E., Manzoni, O. J., & Tonini, R. (2017). Synaptic functions of endocannabinoid signaling in health and disease. In *Neuropharmacology* (Vol. 124, pp. 13–24). Elsevier Ltd. https://doi.org/10.1016/j.neuropharm.2017.06.017

Augustin, S. M., & Lovinger, D. M. (2018). Functional Relevance of Endocannabinoid-Dependent Synaptic Plasticity in the Central Nervous System. In *ACS Chemical Neuroscience* (Vol. 9, Issue 9, pp. 2146–2161). American Chemical Society. https://doi.org/10.1021/acschemneuro.7b00508

Azad, S. C., Kurz, J., Marsicano, G., Lutz, B., Zieglgänsberger, W., & Rammes, G. (2008). Activation of CB1 specifically located on GABAergic interneurons inhibits LTD in the lateral amygdala. *Learn Mem*, *15*(3), 143–152. https://doi.org/10.1101/lm.741908.activity

Bacci, A., Huguenard, J. R., & Prince, D. A. (2004). Long-lasting self-inhibition of neocortical interneurons mediated by endocannabinoids. *Nature*, *431*, 312–316. https://doi.org/10.1038/nature02782.1.

Bellocchio, L., Lafenêtre, P., Cannich, A., Cota, D., Puente, N., Grandes, P., Chaouloff, F., Piazza, P. V., & Marsicano, G. (2010). Bimodal control of stimulated food intake by the endo cannabinoid system. *Nat Neurosci*, *13*(3), 281–283. https://doi.org/10.1038/nn.2494

Best, A. R., & Regehr, W. G. (2008). Serotonin evokes endocannabinoid release and retrogradely suppresses excitatory synapses. *Journal of Neuroscience*, *28*(25), 6508–6515. https://doi.org/10.1523/JNEUROSCI.0678-08.2008

Bilkei-Gorzo, A. (2012). The endocannabinoid system in normal and pathological brain ageing. In *Philosophical Transactions of the Royal Society B: Biological Sciences* (Vol. 367, Issue 1607, pp. 3326–3341). Royal Society. https://doi.org/10.1098/rstb.2011.0388

Bodor, L., Mackie, K., Ledent, C., & Ha, N. (2005). Endocannabinoid Signaling in Rat Somatosensory Cortex : Laminar Differences and Involvement of Specific Interneuron Types. *Journal of Neuroscience*, *25*(29), 6845–6856. https://doi.org/10.1523/JNEUROSCI.0442-05.2005

Brown, S. P., Brenowitz, S. D., & Regehr, W. G. (2003). Brief presynaptic bursts evoke synapse-specific retrograde inhibition mediated by endogenous cannabinoids. *Nature Neuroscience*, *6*(10), 1048–1057. https://doi.org/10.1038/nn1126

Busquets-Garcia, A., Bains, J., & Marsicano, G. (2018). CB 1 Receptor Signaling in the Brain: Extracting Specificity from Ubiquity. In *Neuropsychopharmacology* (Vol. 43, Issue 1, pp. 4–20). Nature Publishing Group. https://doi.org/10.1038/npp.2017.206

Campbell, V. A., & Gowran, A. (2007). Alzheimer's disease; taking the edge off with cannabinoids? In *British Journal of Pharmacology* (Vol. 152, Issue 5, pp. 655–662). https://doi.org/10.1038/sj.bjp.0707446

Cardin, J. A. (2018). Inhibitory Interneurons Regulate Temporal Precision and Correlations in Cortical Circuits. In *Trends in Neurosciences* (Vol. 41, Issue 10, pp. 689–700). Elsevier Ltd. https://doi.org/10.1016/j.tins.2018.07.015

Cass, D. K., Flores-Barrera, E., Thomases, D. R., Vital, W. F., Caballero, A., & Tseng, K. Y. (2014). CB1 cannabinoid receptor stimulation during adolescence impairs the maturation of GABA function in the adult rat prefrontal cortex. *Mol Psychiatry*, *19*(5), 536–543. https://doi.org/10.1038/mp.2014.14

Castillo, P., Younts, T., Chávez, A., & Hashimotodani, Y. (2012). Endocannabinoid Signaling and Synaptic Function. *Neuron*, *76*(1), 70–81. https://doi.org/10.1016/j.neuron.2012.09.020

Chevaleyre, V., & Castillo, P. E. (2003). Heterosynaptic LTD of Hippocampal GABAergic Synapses: A Novel Role of Endocannabinoids in Regulating Excitability. In *Neuron* (Vol. 38).

Chevaleyre, V., Heifets, B. D., Kaeser, P. S., & Su, T. C. (2007). Endocannabinoid-Mediated Long-Term Plasticity Requires cAMP / PKA Signaling and RIM1 a. *Neuron*, *54*(5), 801–812. https://doi.org/10.1016/j.neuron.2007.05.020

Chevaleyre, V., Takahashi, K. A., & Castillo, P. E. (2006). Endocannabinoid-Mediated Synaptic Plasticity in the CNS. *Annu Rev Neurosci*, *29*, 37–76. https://doi.org/10.1146/annurev.neuro.29.051605.112834

Chiu, C. Q., Martenson, J. S., Yamazaki, M., Natsume, R., Sakimura, K., Tomita, S., Tavalin, S. J., & Higley, M. J. (2017). *Input-specific NMDAR-dependent potentiation of dendritic GABAergic inhibition*.

Chiu, C. Q., Puente, N., Grandes, P., & Castillo, P. E. (2010). Dopaminergic modulation of endocannabinoid-mediated plasticity at GABAergic synapses in the prefrontal cortex. *Journal of Neurology*, *30*(21), 7236–7248. https://doi.org/10.1523/JNEUROSCI.0736-10.2010.Dopaminergic

Chiu, Lur, G., Morse, T., Carnevale, N., Ellis-Davies, G., & Higley, M. (2013). Compartmentalization of GABAergic Inhibition by Dendritic Spines. *Science*, *340*(6133), 759–762. https://doi.org/10.1126/science.1234274

Devane, W. A., Hanus, L., Breuer, A., Pertwee, R. G., Stevenson, L. A., Griffin, G., Gibson, D., Mandelbaum, A., & Etinger, A. (1992). Isolation and Structure of a Brain Constituent That Binds to the Cannabinoid Receptor. *Science*, *258*(5090), 1946–1949.

Di Marzo, V., Stella, N., & Zimmer, A. (2015). Endocannabinoid signalling and the deteriorating brain. In *Nature Reviews Neuroscience* (Vol. 16, Issue 1, pp. 30–42). Nature Publishing Group. https://doi.org/10.1038/nrn3876

Díaz-alonso, J., Guzmán, M., & Galve-roperh, I. (2012). Endocannabinoids via CB1 receptors act as neurogenic niche cues during cortical development. *Philos Trans R Soc Lond B Biol Sci*, *367*(1607), 3229–3241. https://doi.org/10.1098/rstb.201

Dumitriu, D., Cossart, R., Huang, J., & Yuste, R. (2007). Correlation between axonal morphologies and synaptic input kinetics of interneurons from mouse visual cortex. *Cerebral Cortex*, *17*(1), 81–91. https://doi.org/10.1093/cercor/bhj126

Földy, C., Neu, A., Jones, M. V., & Soltesz, I. (2006). Presynaptic, activity-dependent modulation of cannabinoid type 1 receptor-mediated inhibition of GABA release. *Journal of Neuroscience*, *26*(5), 1465–1469. https://doi.org/10.1523/JNEUROSCI.4587-05.2006

Freund, F., & Katona, I. (2007). Perisomatic Inhibition. *Neuron*, *56*(1), 33–42. https://doi.org/10.1016/j.neuron.2007.09.012

Fukudome, Y., Ohno-shosaku, T., Matsui, M., Omori, Y., Fukaya, M., Tsubokawa, H., Taketo, M., Watanabe, M., Manabe, T., & Kano, M. (2004). Two distinct classes of muscarinic action on hippocampal inhibitory synapses : M2-mediated direct suppression and M1/M3-mediated indirect suppression through endocannabinoid signalling. *European Journal of Neuroscience*, *19*(10), 2682–2692. https://doi.org/10.1111/j.1460-9568.2004.03384.x

Gabernet, L., Jadhav, S. P., Feldman, D. E., Carandini, M., & Scanziani, M. (2005). Somatosensory integration controlled by dynamic thalamocortical feed-forward inhibition. *Neuron*, *48*(2), 315–327. https://doi.org/10.1016/j.neuron.2005.09.022

Galarreta, M., Erdelyi, F., Szabo, G., & Hestrin, S. (2008). Cannabinoid Sensitivity and Synaptic Properties of 2 GABAergic Networks in the Neocortex. *Cereb Cortex*, *18*(10), 2296–2305. https://doi.org/10.1093/cercor/bhm253

Gerdeman, G. L., Ronesi, J., & Lovinger, D. M. (2002). Postsynaptic endocannabinoid release is critical to long-term depression in the striatum. *Nature Neuroscience*, *5*(5), 446–451. https://doi.org/10.1038/nn832

Gray, J. A., & Roth, B. L. (2007). Molecular targets for treating cognitive dysfunction in schizophrenia. In *Schizophrenia Bulletin* (Vol. 33, Issue 5, pp. 1100–1119). https://doi.org/10.1093/schbul/sbm074

Hashimoto, T., Bazmi, H. H., Mirnics, K., Wu, Q., Sampson, A. R., & Lewis, D. A. (2008). Conserved Regional Patterns of GABA-Related Transcript Expression in the Neocortex of Subjects With Schizophrenia. *Am J Psychiatry*, *165*(4), 479–489. https://doi.org/10.1176/appi.ajp.2007.07081223.

Hashimotodani, Y., Ohno-shosaku, T., & Kano, M. (2007). Presynaptic Monoacylglycerol Lipase Activity Determines Basal Endocannabinoid Tone and Terminates Retrograde Endocannabinoid Signaling in the Hippocampus. *Journal of Neurology*, *27*(5), 1211–1219. https://doi.org/10.1523/JNEUROSCI.4159-06.2007

Hashimotodani, Y., Ohno-shosaku, T., Tsubokawa, H., Ogata, H., Emoto, K., Maejima, T., Araishi, K., Shin, H., & Kano, M. (2005). Phospholipase Cβ Serves as a Coincidence Detector through Its Ca2+ Dependency for Triggering Retrograde Endocannabinoid Signal. *Neuron*, *45*(2), 257–268. https://doi.org/10.1016/j.neuron.2005.01.004

Heifets, B. D., & Castillo, P. E. (2009). Endocannabinoid Signaling and Long-term Synaptic Plasticity. *Annu Rev Physiol*, *71*, 283–306. https://doi.org/10.1146/annurev.physiol.010908.163149.Endocannabinoid

Heifets, B. D., Chevaleyre, V., & Castillo, P. E. (2008). Interneuron activity controls endocannabinoid- mediated presynaptic plasticity through calcineurin. *PNAS*, *105*(29), 10250–10255. https://doi.org/10.1073/pnas.0711880105

Herkenham, M., Lynn, A., Little, M., Johnson, M., Lawrence, S., DeCosta, B., & Rice, K. (1990). Cannabinoid receptor localization in brain. *Proc Natl Acad Sci U S A*, *87*(5), 1932–1936.

Hill, E. L., Gallopin, T., Fe, I., Cauli, B., Rossier, J., Schweitzer, P., El, H., & Gallopin, T. (2007). Functional CB1 Receptors Are Broadly Expressed in Neocortical GABAergic and Glutamatergic Neurons. *J Neurophysiol*, *97*(4), 2580–2589. https://doi.org/10.1152/jn.00603.2006.The

Hillard, C. J., Weinlander, K. M., & Stuhr, K. L. (2012). Contributions of Endocannabinoid Signaling to Psychiatric Disorders in Humans: Genetic and Biochemical Evidence. *Neurocience*, *204*, 207–229. https://doi.org/10.1016/j.neuroscience.2011.11.020

Holley, S. M., Galvan, L., Kamdjou, T., Dong, A., Levine, M. S., & Cepeda, C. (2019). Major contribution of somatostatin-expressing interneurons and cannabinoid receptors to increased GABA synaptic activity in the striatum of Huntington's disease mice. *Frontiers in Synaptic Neuroscience*, *11*(MAY). https://doi.org/10.3389/fnsyn.2019.00014

Howlett, A. C., Barth, F., Bonner, T. I., Cabral, G., Casellas, P., Devane, W. A., Felder, C. C., Herkenham, M., Mackie, K., Martin, B. R., Mechoulam, R., & Pertwee, R. G. (2002). Classification of Cannabinoid Receptors. *Pharmacol Rev*, *54*(2), 161–202.

Hu, H. Y., Kruijssen, D. L. H., Frias, C. P., Rózsa, B., Hoogenraad, C. C., & Wierenga, C. J. (2019). Endocannabinoid Signaling Mediates Local Dendritic Coordination between Excitatory and Inhibitory Synapses. *Cell Reports*, *27*(3), 666-675.e5. https://doi.org/10.1016/j.celrep.2019.03.078

Kano, M., Ohno-Shosaku, T., Hashimotodani, Y., Uchigashima, M., & Watanabe, M. (2009). Endocannabinoid-Mediated Control of Synaptic Transmission. *Physiol Rev*, *89*(1), 309–380. https://doi.org/10.1152/physrev.00019.2008

Katona, I., & Freund, T. F. (2012). Multiple Functions of Endocannabinoid Signaling in the Brain. *Annu Rev Neurosci.*, *35*, 529–558. https://doi.org/10.1146/annurev-neuro-062111-150420.Multiple

Katona, I., Rancz, E., Acsady, L., Ledent, C., Mackie, K., Norbert, H., & Freund, T. (2001). Distribution of CB1 Cannabinoid Receptors in the Amygdala and their Role in the Control of GABAergic Transmission. *Journal of Neuroscience*, *21*(23), 9506–9518.

Katona, I., Sperlagh, B., Magloczky, Z., Santha, E., Kofalvi, A., Czirjak, S., Mackie, K., Vizi, E. S., & Freund, T. F. (2000). Gabaergic interneurons are the targets of cannabinoid actions in the human hippocampus. *Neuroscience*, *100*(4), 797–804.

Katona, I., Urbán, G., Wallace, M., Ledent, C., Piomelli, D., Mackie, K., & Freund, T. (2006). Molecular Composition of the Endocannabinoid System at Glutamatergic Synapses. *Journal of Neuroscience*, *26*(21), 5628–5637.

Kepecs, A., & Fishell, G. (2014). Interneuron cell types are fit to function. *Nature*, *505*(7483), 318–326. https://doi.org/10.1038/nature12983

Kim, J., & Alger, B. E. (2010). Reduction in endocannabinoid tone is a homeostatic mechanism for specific inhibitory synapses. *Nature Neuroscience*, *13*(5), 592–600. https://doi.org/10.1038/nn.2517

Kishimoto, Y., & Kano, M. (2006). Endogenous Cannabinoid Signaling through the CB 1 Receptor Is Essential for Cerebellum-Dependent Discrete Motor Learning. *Journal of Neuroscience*, *26*(34), 8829–8837. https://doi.org/10.1523/JNEUROSCI.1236-06.2006

Kreitzer, A. C., & Malenka, R. C. (2005). Dopamine Modulation of State-Dependent Endocannabinoid Release and Long-Term Depression in the Striatum. *Journal of Neuroscience*, *25*(45), 10537–10545. https://doi.org/10.1523/JNEUROSCI.2959-05.2005

Lafourcade, M., Elezgarai, I., Mato, S., Bakiri, Y., Grandes, P., & Manzoni, O. J. (2007). Molecular Components and Functions of the Endocannabinoid System in Mouse Prefrontal Cortex. *PLoS One*, *2*(8), e709. https://doi.org/10.1371/journal.pone.0000709

Letzkus, J. J., Wolff, S. B. E., & Lüthi, A. (2015). Disinhibition, a Circuit Mechanism for Associative Learning and Memory. In *Neuron* (Vol. 88, Issue 2, pp. 264–276). Cell Press. https://doi.org/10.1016/j.neuron.2015.09.024

Liu, X., Dimidschstein, J., Fishell, G., & Carter, A. G. (2020). Hippocampal inputs engage cck+ interneurons to mediate endocannabinoid-modulated feed-forward inhibition in the prefrontal cortex. *ELife*, *9*, 1–22. https://doi.org/10.7554/eLife.55267

Lovett-Barron, M., Turi, G. F., Kaifosh, P., Lee, P. H., Bolze, F., Sun, X. H., Nicoud, J. F., Zemelman, B. V., Sternson, S. M., & Losonczy, A. (2012). Regulation of neuronal input transformations by

tunable dendritic inhibition. *Nature Neuroscience*, *15*(3), 423–430. https://doi.org/10.1038/nn.3024

Mackie, K. (2005). Distribution of Cannabinoid Receptors in the Central and Peripheral Nervous System. In *HEP* (Vol. 168). Springer-Verlag.

Maejima, T., Hashimoto, K., Yoshida, T., Aiba, A., & Kano, M. (2001). Presynaptic Inhibition Caused by Retrograde Signal from Metabotropic Glutamate to Cannabinoid Receptors. *Neuron*, *31*, 463–475.

Marrs, W. R., Blankman, J. L., Horne, E. A., Thomazeau, A., Lin, Y. H., Coy, J., Bodor, A. L., Muccioli, G. G., Hu, S. S., Woodruff, G., Fung, S., Lafourcade, M., Alexander, J. P., Long, J. Z., Li, W., Xu, C., Möller, T., Mackie, K., Manzoni, O. J., … Stella, N. (2010). The serine hydrolase ABHD6 controls the accumulation and efficacy of 2-AG at cannabinoid receptors. *Nature Neuroscience*, *13*(8), 951–957. https://doi.org/10.1038/nn.2601

Marsicano, G., & Lutz, B. (1999). *Expression of the cannabinoid receptor CB1 in distinct neuronal subpopulations in the adult mouse forebrain*. https://doi.org/10.1046/j.1460-9568.1999.00847.x

Marsicano, G., Wotjak, C. T., & Azad, S. C. (2002). The endogenous cannabinoid system controls extinction of aversive memories. *Nature*, *418*, 530–534. https://doi.org/10.1038/nature00839

Mato, S., Lafourcade, M., Robbe, D., Bakiri, Y., & Manzoni, O. J. (2007). Role of the cyclic-AMP/PKA cascade and of P/Q-type Ca+2 channels in endocannabinoid-mediated long-term depression in the nucleus accumbens. *Neuropharmacology*, *54*(2008), 87–94. https://doi.org/10.1016/j.neuropharm.2007.04.014

Mcgarry, L. M., Packer, A. M., Fino, E., Nikolenko, V., Sippy, T., & Yuste, R. (2010). Quantitative classification of somatostatin-positive neocortical interneurons identifi es three interneuron subtypes. *Front Neural Circuits*, *4*(12), 1–19. https://doi.org/10.3389/fncir.2010.00012

Mechoulam, R. et al. (1995). Identification of An Endogenous 2-Monoglyceride, Present In Canine Gut, That Binds To Cannabinoid Receptors. *Biochemical Pharmacology*, *50*(1), 83–90.

Michael C.Crair and Robert C.Malenka. (1995). A critical period for long-term potentiation at thalamocortical synapses. *Nature*, *375*, 325–328.

Monory, K., Massa, F., Egertová, M., Eder, M., Blaudzun, H., Westenbroek, R., Kelsch, W., Jacob, W., Marsch, R., Ekker, M., Long, J., Rubenstein, J. L., Goebbels, S., Nave, K. A., During, M., Klugmann, M., Wölfel, B., Dodt, H. U., Zieglgänsberger, W., … Lutz, B. (2006). The Endocannabinoid System Controls Key Epileptogenic Circuits in the Hippocampus. *Neuron*, *51*(4), 455–466. https://doi.org/10.1016/j.neuron.2006.07.006

Munro, S., Thomas, K., & Abu-Shaar, M. (1993). Molecular characterization of a peripheral receptor for cannabinoids. *Nature*, *365*(6441), 61–65. https://doi.org/10.1038/365061a0

Neu, A., Földy, C., & Soltesz, I. (2007). Postsynaptic origin of CB1-dependent tonic inhibition of GABA release at cholecystokinin-positive basket cell to pyramidal cell synapses in the CA1

region of the rat hippocampus. *Journal of Physiology*, *578*(1), 233–247. https://doi.org/10.1113/jphysiol.2006.115691

Ohno-Shosaku, T., & Kano, M. (2014). Endocannabinoid-mediated retrograde modulation of synaptic transmission. In *Current Opinion in Neurobiology* (Vol. 29, pp. 1–8). Elsevier Ltd. https://doi.org/10.1016/j.conb.2014.03.017

Ohno-shosaku, T., Tsubokawa, H., Mizushima, I., Yoneda, N., & Zimmer, A. (2002). Presynaptic Cannabinoid Sensitivity Is a Major Determinant of Depolarization-Induced Retrograde Suppression at Hippocampal Synapses. *Journal of Neuroscience*, *22*(10), 3864–3872.

Pouille, F., Marin-Burgin, A., Adesnik, H., Atallah, B. V., & Scanziani, M. (2009). Input normalization by global feedforward inhibition expands cortical dynamic range. *Nature Neuroscience*, *12*(12), 1577–1585. https://doi.org/10.1038/nn.2441

Pryce, G., Ahmed, Z., Hankey, D. J. R., Jackson, S. J., Croxford, J. L., Pocock, J. M., Ledent, C., Petzold, A., Thompson, A. J., Giovannoni, G., Cuzner, M. L., & Baker, D. (2003). Cannabinoids inhibit neurodegeneration in models of multiple sclerosis. *Brain*, *126*(10), 2191–2202. https://doi.org/10.1093/brain/awg224

Puighermanal, E., Marsicano, G., Busquets-garcia, A., Lutz, B., & Maldonado, R. (2009). Cannabinoid modulation of hippocampal long-term memory is mediated by mTOR signaling. *Nature Neuroscience*, *12*(9). https://doi.org/10.1038/nn.2369

Pytliak, M., Vargová, V., Mechírová, V., & Felšci, M. (2011). Serotonin receptors - from molecular biology to clinical applications. In *Physiological Research* (Vol. 60, Issue 1, pp. 15–25). Czech Academy of Sciences. https://doi.org/10.33549/physiolres.931903

Rudy, B., Fishell, G., Lee, S., & Hjerling-Leffler, J. (2011). Three Groups of Interneurons Account for Nearly 100% of Neocortical GABAergic Neurons. *Dev Neurobiol.*, *71*(1), 45–61. https://doi.org/10.1002/dneu.20853.Three

Saez, T., Aronne, M., Caltana, L., & Brusco, A. (2014). Prenatal exposure to the CB1 and CB2 cannabinoid receptor agonist WIN 55,212-2 alters migration of early-born glutamatergic neurons and GABAergic interneurons in the cerebral cortex. *JOURNAL OF NEUROCHEMISTRY*, *129*(4), 637–648. https://doi.org/10.1111/jnc.12636

Safo, P. K., & Regehr, W. G. (2005). Endocannabinoids control the induction of cerebellar LTD. *Neuron*, *48*(4), 647–659. https://doi.org/10.1016/j.neuron.2005.09.020

Sewell, R. A., Ranganathan, M., & Souza, D. C. D. (2009). Cannabinoids and psychosis. *International Review of Psychiatry*, *21*(April), 152–162. https://doi.org/10.1080/09540260902782802

Sugiura, T., Kobayashi, Y., Oka, S., & Waku, K. (2002). Biosynthesis and degradation of anandamide and 2-arachidonoylglycerol and their possible physiological significance. *Prostaglandins Leukot Essent Fatty Acids*, *66*(2–3), 173–192. https://doi.org/10.1054/plef.2001.0356

Tanimura, A., Uchigashima, M., Yamazaki, M., Uesaka, N., Mikuni, T., & Abe, M. (2012). Synapse type-independent degradation of the endocannabinoid 2-arachidonoylglycerol after

retrograde synaptic suppression. *PNAS*, *109*(30), 12195–12200. https://doi.org/10.1073/pnas.1204404109

Terzian, A., Micale, V., & Wotjak, C. (2014). Cannabinoid receptor type 1 receptors on GABAergic vs . glutamatergic neurons differentially gate sex-dependent social interest in mice. *European Journal of Neuroscience*, *40*, 2293–2298. https://doi.org/10.1111/ejn.12561

Tsou, K., & Mackie, K. (1999). Cannabinoid CB1 Receptors Are Localized Primarily On Cholecystokinin-Containing Gabaergic Interneurons In The Rat Hippocampal Formation. *Neurocience*, *93*(3), 969–975.

Udakis, M., Pedrosa, V., Chamberlain, S. E. L., Clopath, C., & Mellor, J. R. (2020). Interneuron-specific plasticity at parvalbumin and somatostatin inhibitory synapses onto CA1 pyramidal neurons shapes hippocampal output. *Nature Communications*, *11*(1). https://doi.org/10.1038/s41467-020-18074-8

Varma, N., Carlson, G. C., Ledent, C., & Alger, B. E. (2001). *Metabotropic Glutamate Receptors Drive the Endocannabinoid System in Hippocampus*. http://www.jneurosci.org/cgi/content/full/5899

Venkatachalam, K., & Montell, C. (2007). TRP channels. In *Annual Review of Biochemistry* (Vol. 76, pp. 387–417). https://doi.org/10.1146/annurev.biochem.75.103004.142819

Xue, M., Atallah, B. V., & Scanziani, M. (2014). Equalizing excitation-inhibition ratios across visual cortical neurons. *Nature*, *511*(7511), 596–600. https://doi.org/10.1038/nature13321

Yoshida, T., Fukaya, M., Uchigashima, M., Miura, E., Kamiya, H., Kano, M., & Watanabe, M. (2006). Localization of diacylglycerol lipase-α around postsynaptic spine suggests close proximity between production site of an endocannabinoid, 2-arachidonoyl-glycerol, and presynaptic cannabinoid CB1 receptor. *Journal of Neuroscience*, *26*(18), 4740–4751. https://doi.org/10.1523/JNEUROSCI.0054-06.2006

Zou, S., & Kumar, U. (2015). Colocalization of cannabinoid receptor 1 with somatostatin and neuronal nitric oxide synthase in rat brain hippocampus. *Brain Research*, *1622*, 114–126. https://doi.org/10.1016/j.brainres.2015.06.021

Zou, S., & Kumar, U. (2018). Cannabinoid receptors and the endocannabinoid system: Signaling and function in the central nervous system. In *International Journal of Molecular Sciences* (Vol. 19, Issue 3). MDPI AG. https://doi.org/10.3390/ijms19030833

APPENDANT

Table 1

Figure 3: WIN effect	**Normality Test (Shapiro-Wilk-Test)**	**Test used**	**N**	**P value**
SOM-Cre v/s PV-Cre	pass	Unpaired t-test	7	$p < 0.0001$
PPR SOM-Cre	pass	Paired t-test	7	0.0006
PPR PV-Cre	pass	Paired t-test	6	0.2675
Figure 4: WIN effect	**Normality Test (Shapiro-Wilk-Test)**	**Test used**	**N**	**P value**
SOM-Cre v/s AM251	pass	Unpaired t-test	7	$p < 0.0001$
PPR SOM-Cre	pass	Paired t-test	7	0.0076
PPR AM251	pass	Paired t-test	7	0.2379
Figure 5: Short-Term Depression	**Normality Test (Shapiro-Wilk-Test)**	**Test used**	**N**	**P value**
PPR SOM-Cre	pass	Paired t-test	7	0.0017
PPR PV-Cre	pass	Paired t-test	4	0.1521
Figure 6: Short-Term Depression	**Normality Test (Shapiro-Wilk-Test)**	**Test used**	**N**	**P value**
PPR SOM-Cre	pass	Paired t-test	8	0.0006
PPR AM251	pass	Paired t-test	7	0.0906
Figure 7: Long-Term Depression	**Normality Test (Shapiro-Wilk-Test)**	**Test used**	**N**	**P value**
SOM-Cre v/s PV-Cre	pass	Unpaired t-test	7	<0.0001
PPR SOM-Cre	pass	Paired t-test	7	0.0004
PPR PV-Cre	pass	Paired t-test	6	0.3856
Figure 8: Long-Term Depression	**Normality Test (Shapiro-Wilk-Test)**	**Test used**	**N**	**P value**

SOM-Cre v/s AM251	pass	Unpaired t-test	7	<0.0001
PPR SOM-Cre	pass	Paired t-test	7	0.0054
PPR AM251	No passed	Wilcoxon matched pairs signed rank test	7	0.9375
Figure 9: Long-Term Depression	**Normality Test (Shapiro-Wilk-Test)**	**Test used**	**N**	**P value**
SOM-Cre v/s GDPβS	pass	Unpaired t-test	6	<0.0001
PPR SOM-Cre	pass	Paired t-test	8	0.0019
PPR GDPβS	No passed	Wilcoxon matched pairs signed rank test	7	0.3750
Figure 10: Long-Term Depression	**Normality Test (Shapiro-Wilk-Test)**	**Test used**	**N**	**P value**
SOM-Cre v/s BAPTA	pass	Unpaired t-test	6	<0.0001
SOM-Cre v/s MCPG	pass	Unpaired t-test	6	<0.0001
PPR BAPTA	pass	Paired t-test	7	0.7850
PPR MCPG	pass	Paired t-test	7	0.2085
Figure 11: 5HT effect	**Normality Test (Shapiro-Wilk-Test)**	**Test used**	**N**	**P value**
SOM-Cre v/s PV-Cre	pass	Unpaired t-test	6	<0.0001
PPR SOM-Cre	pass	Paired t-test	6	0.0681
PPR PV-Cre	pass	Paired t-test	4	0.9829
Figure 12: TCB2 effect	**Normality Test (Shapiro-Wilk-Test)**	**Test used**	**N**	**P value**
SOM-Cre v/s PV-Cre	pass	Unpaired t-test	6	<0.0001
PPR SOM-Cre	No passed	Wilcoxon matched pairs signed rank test	5	0.0625

PPR PV-Cre	N too small	N too small		
Figure 13: Long-Term Depression	**Normality Test (Shapiro-Wilk-Test)**	**Test used**	**N**	**P value**
SOM-Cre v/s Ritanserin	pass	Unpaired t-test	7	<0.0001
PPR SOM-Cre	pass	Paired t-test	7	0.0063
PPR Ritanserin	pass	Paired t-test	3	0.3048

Table 2

Figure 14: WIN effect	**Normality Test (Shapiro-Wilk-Test)**	**Test used**	**N**	**P value**
SOM-Cre v/s SOMCB1KO	pass	Unpaired t-test	7	<0.0001
PPR SOM-Cre v/s SOMCB1KO	pass	Unpaired t-test	7	0.0413
Figure 15: 5-HT effect	**Normality Test (Shapiro-Wilk-Test)**	**Test used**	**N**	**P value**
SOM-Cre v/s SOMCB1KO	pass	Unpaired t-test	6	<0.0001
PPR SOM-Cre	pass	Paired t-test	6	0.0681
PPR SOMCB1KO	pass	Paired t-test	5	0.4526
Figure 16: TCB2 effect	**Normality Test (Shapiro-Wilk-Test)**	**Test used**	**N**	**P value**
SOM-Cre v/s SOMCB1KO	pass	Unpaired t-test	6	<0.0001
PPR SOM-Cre	No passed	Wilcoxon matched pairs signed rank test	5	0.0625
PPR SOMCB1KO	pass	Paired t-test	5	0.8948
Figure 17: Short-Term Depression	**Normality Test (Shapiro-Wilk-Test)**	**Test used**	**N**	**P value**
PPR SOM-Cre	pass	Paired t-test	7	0.0033
PPR SOMCB1KO	pass	Paired t-test	8	0.0925

Figure 18: Long-Term Depression	**Normality Test (Shapiro-Wilk-Test)**	**Test used**	**N**	**P value**
SOM-Cre v/s SOMCB1KO	pass	Unpaired t-test	7	<0.0001
PPR SOM-Cre	pass	Paired t-test	7	0.0008
PPR SOMCB1KO	No passed	Wilcoxon matched pairs signed rank test	9	0.6328
Figure 19: Input-Ouput Inhibitory response	**Normality Test (Shapiro-Wilk-Test)**	**Test used**	**N**	**P value**
20V Control v/s SOMCB1KO	pass	one-way ANOVA, Sidak's multiple comparisons test	10	0.7219
30V Control v/s SOMCB1KO	pass	one-way ANOVA, Sidak's multiple comparisons test	10	0.6000
40V Control v/s SOMCB1KO	pass	one-way ANOVA, Sidak's multiple comparisons test	10	0.0087
50V Control v/s SOMCB1KO	pass	one-way ANOVA, Sidak's multiple comparisons test	10	0.0416
60V Control v/s SOMCB1KO	pass	one-way ANOVA, Sidak's	10	0.0035

		multiple comparisons test		
70V Control v/s SOMCB1KO	pass	one-way ANOVA, Sidak's multiple comparisons test	10	0.0010
80V Control v/s SOMCB1KO	pass	one-way ANOVA, Sidak's multiple comparisons test	10	<0.0001
Figure 20: Spontaneous Inhibitory transmission	**Normality Test (Shapiro-Wilk-Test)**	**Test used**	**N**	**P value**
sIPSC frequency Control v/s SOMCB1KO	pass	Unpaired t-test	10	0.0369
sIPSC amplitude Control v/s SOMCB1KO	pass	Unpaired t-test	10	0.2940
Figure 21: Input-Ouput Excitatory response	**Normality Test (Shapiro-Wilk-Test)**	**Test used**	**N**	**P value**
20V Control v/s SOMCB1KO	pass	one-way ANOVA, Sidak's multiple comparisons test	9	0.7077
30V Control v/s SOMCB1KO	pass	one-way ANOVA, Sidak's multiple comparisons test	9	0.1923

40V Control v/s SOMCB1KO	pass	one-way ANOVA, Sidak's multiple comparisons test	9	0.0146
50V Control v/s SOMCB1KO	pass	one-way ANOVA, Sidak's multiple comparisons test	9	0.0001
60V Control v/s SOMCB1KO	pass	one-way ANOVA, Sidak's multiple comparisons test	9	p<0.0001
70V Control v/s SOMCB1KO	pass	one-way ANOVA, Sidak's multiple comparisons test	9	p<0.0001
80V Control v/s SOMCB1KO	pass	one-way ANOVA, Sidak's multiple comparisons test	9	p<0.0001
90V Control v/s SOMCB1KO	pass	one-way ANOVA, Sidak's multiple comparisons test	9	p<0.0001
PPR Control v/s SOMCB1KO	pass	Unpaired t-test	9	0.0117
E/I Ratio Control v/s SOMCB1KO	pass	Unpaired t-test	9	0.8260

Figure 22: Spontaneous excitatory transmission	**Normality Test (Shapiro-Wilk-Test)**	**Test used**	**N**	**P value**
sEPSC frequency Control v/s SOMCB1KO	No passed	Mann Whitney test	9	0.0016
sEPSC amplitude Control v/s SOMCB1KO	pass	Unpaired t-test	9	0.2814
Figure 23: Action potential evoked	**Normality Test (Shapiro-Wilk-Test)**	**Test used**	**N**	**P value**
AP firing threshold Control v/s SOMCB1KO	No passed	Mann Whitney test	6	0.0006
Half Intensity Control v/s SOMCB1KO	No passed	Mann Whitney test	6	0.0006
Figure 24: Probability of evoking Action Potential at 30V	**Normality Test (Shapiro-Wilk-Test)**	**Test used**	**N**	**P value**
1° pulse Control v/s SOMCB1KO	No passed	Two-way ANOVA Sidak's multiple comparisons test	6	<0.0001
2° pulse Control v/s SOMCB1KO	No passed	Two-way ANOVA Sidak's multiple comparisons test	6	0.1189
3° pulse Control v/s SOMCB1KO	No passed	Two-way ANOVA Sidak's multiple comparisons test	6	0.9992
4° pulse Control v/s SOMCB1KO	No passed	Two-way ANOVA Sidak's multiple comparisons test	6	>0.9999
5° pulse Control v/s SOMCB1KO	No passed	Two-way ANOVA	6	0.9992

		Sidak's multiple comparisons test		
Figure 25: Probability to evoke Action Potential at half-intensity	**Normality Test (Shapiro-Wilk-Test)**	**Test used**	**N**	**P value**
1° pulse Control v/s SOMCB1KO	No passed	Two-way ANOVA Sidak's multiple comparisons test	6	>0.9999
2° pulse Control v/s SOMCB1KO	No passed	Two-way ANOVA Sidak's multiple comparisons test	6	0.0009
3° pulse Control v/s SOMCB1KO	No passed	Two-way ANOVA Sidak's multiple comparisons test	6	0.9934
4° pulse Control v/s SOMCB1KO	No passed	Two-way ANOVA Sidak's multiple comparisons test	6	>0.9999
5° pulse Control v/s SOMCB1KO	No passed	Two-way ANOVA Sidak's multiple comparisons test	6	0.9983
Figure 26: Intrinsic properties Control v/s SOMCB1KO	**Normality Test (Shapiro-Wilk-Test)**	**Test used**	**N**	**P value**
Figure E: Threshold membrane potential (mV)	pass	Unpaired t-test	7	0.8133
Figure F: Half-width (ms)	pass	Unpaired t-test	7	0.3383
Figure G: Rheobase (pA)	pass	Unpaired t-test	7	0.6102
Figure H: Interevent-Interval (ms)	pass	Unpaired t-test	7	0.7349